

Cone signal interactions in direction-selective neurons in the middle temporal area

Crista L. Barberini

Department of Neurobiology, Stanford University, Stanford, CA, USA



Marlene R. Cohen

Department of Neurobiology, Stanford University, Stanford, CA, USA



Brian A. Wandell

Department of Psychology, Stanford University, Stanford, CA, USA



William T. Newsome

Department of Neurobiology and Howard Hughes Medical Institute, Stanford University, Stanford, CA, USA



Many experimental measurements support the hypothesis that the middle temporal (MT) area of the rhesus monkey has a central role in processing visual motion. Most of these studies were performed using luminance stimuli, leaving open the question of how color information is used during motion processing. We investigated the specific question of how S-cone signals, an important source of color information, interact with L,M-cone signals, the dominant source of luminance information. In the MT area, S-cone-initiated signals combine synergistically with L,M-cone (luminance) signals over most of the stimulus range, regardless of whether the stimuli are added or subtracted. A quantitative analysis of the responses to the combination of S- and L,M-cone signals shows that for a significant minority of cells, these S-cone signals are carried to the MT area by a color-opponent (“blue-yellow”) pathway, such that in certain limited contrast ranges, a small amount of S- and L,M-cone cancellation is observed. Both S- and L,M-cone responses are direction-selective, suggesting that MT processes a wide range of motion signals, including those carried by luminance and color. To investigate this possibility further, we measured MT responses while monkeys discriminated the direction of motion of luminance and S-cone-initiated gratings. The sensitivity of single MT neurons and the correlation between trial-to-trial variations in single neuron firing and perception are similar for S- and L,M-cone stimuli, further supporting a role for the MT area in processing chromatic motion.

Keywords: color; motion; MT; macaque; vision; cones

Introduction

The middle temporal (MT) area of the rhesus monkey has a central role in the processing of visual motion (Britten, Shadlen, Newsome, & Movshon, 1992; Chawla, Phillips, Buechel, Edwards, & Friston, 1998; Gegenfurtner et al., 1994; Maunsell & Van Essen, 1983; Zeki, 1974; Zeki et al., 1991). Mainly, this role has been documented using luminance motion stimuli, in keeping with the strong luminance input the MT area receives via the magnocellular pathway (Maunsell, Nealey, & DePriest, 1990). In previous decades, the apparent absence of color responsivity in the MT area (Maunsell & Van Essen, 1983; Van Essen, Maunsell, & Bixby, 1981; Zeki, 1978b) and the limited input from visual pathways carrying chromatic information led some researchers to hypothesize that the MT area is not involved in the processing of chromatic motion. Various proposals were entertained, ranging from the possibility that color motion

is not perceived or that it is processed elsewhere in the brain (Gegenfurtner et al., 1994; Livingstone & Hubel, 1987; Maunsell & Newsome, 1987; Zeki, 1976, 1978a).

It is now clear that color motion is perceived. Furthermore, several recent studies have documented MT responses to chromatic motion and raised the possibility that the MT area contains signals suitable for processing both luminance and chromatically defined motion (Dobkins & Albright, 1994; Gegenfurtner et al., 1994; Saito, Tanaka, Isono, Yasuda, & Mikami, 1989; Seidemann, Poirson, Wandell, & Newsome, 1999; Thiele, Dobkins, & Albright, 2001). However, the chromatic signals in the MT area have not been characterized by a quantitative model that might be compared with psychophysical performance.

We, therefore, undertook an assessment of cone interactions in isolated neurons in the MT area, measuring how responses to S-cone drifting gratings change when L,M-cone contrast is added in phase and out of phase to the stimulus. Here, we introduce a quantitative model of the

62 responses of the MT neurons to chromatic stimuli, and we
 63 evaluate the model's performance against the data. We
 64 then characterize the relationship between S-cone
 65 responses in the MT area and chromatic motion perception
 66 by recording single unit activity while a monkey discrim-
 67 inates the direction of motion in S-cone and luminance
 68 Gabor stimuli. We quantify the neural sensitivity to motion
 69 in these stimuli and compare it to the simultaneously
 70 measured psychophysical sensitivity. We also assess the
 71 trial-by-trial correlation of variability in these neural
 72 responses with the monkey's perceived direction of motion.
 73 We find that (1) for the most part, S-cone-initiated
 74 signals combine positively with L,M-cone signals, such
 75 that the response initiated by an S-cone signal is never
 76 entirely canceled by the addition of an L,M-cone signal;
 77 (2) S-cone signals arrive in the MT area via pathways that
 78 are both color-opponent and summative with L,M-cone
 79 signals; (3) neural sensitivity to motion initiated in S-cone
 80 signals is roughly equal to psychophysical sensitivity; and
 81 (4) responses of MT neurons are correlated on a trial-by-
 82 trial basis with the monkey's perception of motion initiated
 83 in S cones.

Theoretical background

85 We measured and modeled the responses of single
 86 neurons to a set of stimuli designed to reveal how S-cone
 87 signals combine with L,M-cone signals in the MT area. The
 88 stimuli were sums and differences of S- and L,M-cone
 89 gratings presented at a range of contrasts. This set of
 90 stimuli is depicted in a grid in Figure 1. In this figure,
 91 L,M-cone contrast varies along the horizontal axis and
 92 S-cone contrast along the vertical axis. The L,M-cone stimuli
 93 are created by adding equal contrast L- and M-cone stimuli

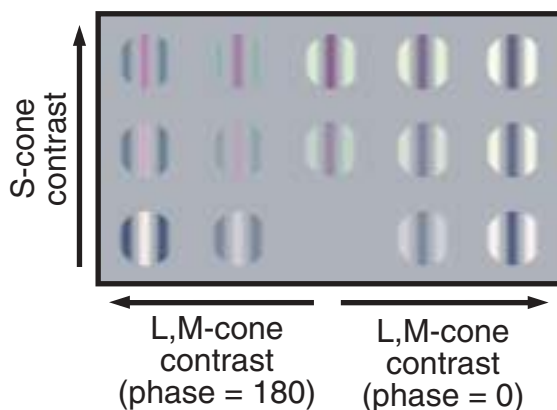


Figure 1. Stimulus space. Stimuli consisted of sine-wave gratings or Gabors containing varying levels of L,M- and S-cone contrast, added either in phase (right half) or out of phase (left half). The stimulus set gives rise to a grid of trial conditions. Approximations of some of the stimuli are placed within this grid. Neural responses are plotted in this space in subsequent figures.

in the same spatial and temporal phase; these are luminance
 94 stimuli. Positive L,M-cone values describe conditions in
 95 which the L,M-cone stimulus is combined in phase with the
 96 S-cone stimulus (i.e., added), whereas negative values
 97 describe conditions in which the L,M-cone stimulus is
 98 combined out-of-phase with the S-cone stimulus (i.e.,
 99 subtracted). In Figure 1, examples of how the gratings
 100 would appear are placed within this space. 101

Figure 2 illustrates the responses of an MT neuron as the
 102 stimulus varied across the space in Figure 1. The surface
 103 height and color in Figure 2A indicate the response mag-
 104 nitude. The three curves in Figure 2B are slices through this
 105 surface at constant S-cone contrast levels. The main fea-
 106 tures of the neural responses illustrated in this figure were
 107 present consistently across MT neurons, and these features
 108

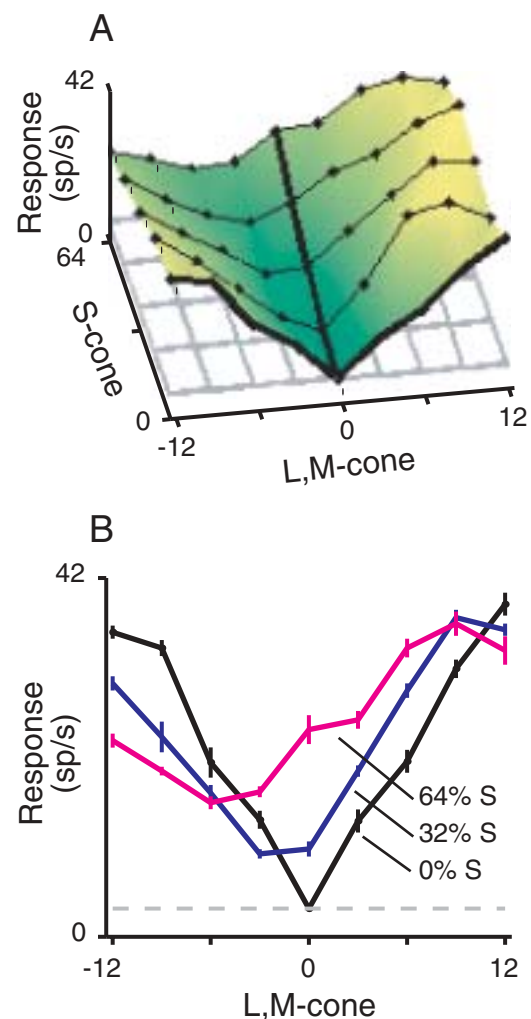


Figure 2. Neural response profile for one neuron. (A). Three-dimensional surface plot of the neural response to the grid of stimuli. Heavy lines highlight the purely L,M- and S-cone contrast response functions. The color scale indicates relative response amplitude, running from zero (dark green) to the maximum firing rate (bright yellow). (B). Two-dimensional slices through the neural response profile at three S-cone contrast levels. Error bars are standard error of the mean.

109 provide the theoretical basis for our model of MT neuronal
 110 responses. First, as L,M-cone contrast is added to or
 111 subtracted from an S-cone stimulus, the response magni-
 112 tude generally increases. Second, there is a small amount of
 113 response cancellation. Over a small contrast region, adding
 114 L,M-cone contrast to a particular S-cone stimulus elicits a
 115 response minimum at a nonzero L,M-cone contrast level
 116 (e.g., [Figure 2B](#), 64% S curve). However, this response
 117 cancellation is a relatively small effect; adding or subtract-
 118 ing L,M-cone contrast to an S-cone stimulus almost never
 119 drives the response back to baseline. Third, the neural
 120 responses saturate at higher contrast levels.

121 We capture these three properties of the data in a model
 122 of MT neural signals that focuses on how cone inputs
 123 interact to drive the neural response. The model predicts
 124 neural firing rate as a function of cone contrast. We refer to
 125 the S-cone contrast as s , and to the (equal) L,M-cone
 126 contrasts as k . We refer to the number of action potentials
 127 per second as r . The relationship between stimulus contrast
 128 and number of action potentials is

$$r = F(s, k). \quad (1)$$

129 Our first specification of the model reflects the fact that
 130 both adding and subtracting L,M-cone contrast to any level
 131 of S-cone contrast generally increases the response. We
 132 therefore represent the response function as comprising two
 133 positive terms (and here add a variable, a , for the sponta-
 134 neous firing rate):

$$r = |F_1(s)| + |F_2(k)| + a. \quad (2)$$

135 A second critical feature of the neural response concerns
 136 the location of the minimum response as L,M-cone con-
 137 trast is added to a fixed S-cone contrast. In the absence of
 138 S-cone contrast, the L,M-cone contrast response function
 139 is symmetric about zero. However, in the presence of some
 140 level of S-cone contrast, for some neurons (e.g., [Figure 2B](#)),
 141 the response minimum shifts slightly toward negative L,M-
 142 cone contrasts. This asymmetry or an asymmetry of the
 143 opposite sign (i.e., a response minimum at a positive L,M-
 144 cone contrast) was evident in many of the MT neurons we
 145 recorded. [Equation 2](#) cannot account for this. We incorpo-
 146 rate this response feature into the model by assuming that
 147 $F_1(\cdot)$ depends on a weighted sum of s and k . Hence, we
 148 modify the equation by introducing a dependence on k into
 149 the first term:

$$r = |F_1(s, k)| + |F_2(k)| + a. \quad (3)$$

150 To complete the model, we must define the functions F_i
 151 that relate stimulus contrast to response. The general form
 152 of the contrast response functions in these experiments is
 153 common in MT cells and many other cortical visual neu-
 154 rons (Carandini, Heeger, & Movshon, [1997](#); Simoncelli &

Heeger, [1998](#)). We model this relationship using a conven-
 tional contrast normalization expression:

$$F_1(x) = m_i \frac{x}{\sqrt{c_i + x^2}}. \quad (4)$$

The equation contains one variable, x , which is contrast,
 and two parameters. The parameters are m_i , which is
 response magnitude, and c_i , which is most often called
 the semisaturation constant. These parameters are con-
 strained to be positive. Inserting the contrast function into
[Equation 3](#), along with a scaling parameter b , which
 describes the relative influence of s and k within the left
 hand term, completes the response model:

$$r = m_1 \left| \frac{s + bk}{\sqrt{c_1 + (s + bk)^2}} \right| + m_2 \left| \frac{k}{\sqrt{c_2 + k^2}} \right| + a. \quad (5)$$

This response model is the basis for our quantitative
 analysis of how S- and L,M-cone modulations determine
 the responses of MT neurons. Each of the model parameters
 summarizes a simple property of the neural response. The
 positive semisaturation constants characterize the contrast
 response properties of the two types of input signals. The
 positive coefficients characterize the relative significance
 of the cone inputs to the response.

The coefficient b is of particular theoretical significance
 for evaluating whether color opponency is evident in the
 neural response. When b is zero, the model is purely
 symmetric and does not exhibit the lateral shift of the
 response minimum as S-cone contrast increases. When b is
 positive, however, S- and L,M-cone inputs sum, and the
 response minimum occurs when S- and L,M-cone signals
 are subtracted from each other (i.e., the stimuli are out-of-
 phase), yielding a response minimum to the left of zero
 (e.g., [Figure 2](#)). Conversely, a negative value of b indicates
 opponent interactions between S- and L,M-cone signals,
 and the response minimum shifts to the right of zero (see
[Results](#)). A significant portion of our analysis focuses on
 measuring the sign and value of this parameter and under-
 standing its distribution across our sample of MT neurons.

We tested other models of the neural response, including
 a standard polynomial equation, and a series of exponen-
 tials, one for each level of S-cone contrast, offset by a
 certain amount. We also tested other versions of the cone-
 interaction model. We settled on the model in [Equation 5](#)
 because (a) it was optimal in terms of being able to
 interpret fitted parameter values physiologically, (b) it
 had the fewest number of free parameters, and (c) the
 results, including the percentage of neurons exhibiting
 opponency or summation, did not change qualitatively for
 any of the other models.

Note that our paradigm is more than a standard re-
 sponse minimization or color mixture experiment; rather,

201 it represents an extensive examination of the cone interac-
 202 tions. By running a full grid of cone contrast combinations,
 203 we measure color across a broad range of neural responses.
 204 This approach allows us to model the cone interactions
 205 much more completely than measurements restricted to
 206 estimating a single point in this grid (isoluminant) or the
 207 neural responses to any single contrast series (a single line
 208 through this grid).

209 Methods

210 We conducted experiments in two adult rhesus monkeys
 211 (*Macaca mulatta*, both female, weight 7–10 kg). Before the
 212 experiments, we surgically implanted each animal with a
 213 head-holding device (Evarts, 1968), a scleral search coil
 214 for measuring eye movements (Judge, Richmond, & Chu,
 215 1980), and a recording cylinder (Crist Instruments, Damascus,
 216 MD) that provided access to the MT area. During experi-
 217 ments, the animals sat in a primate chair with their heads
 218 restrained, facing a CRT display. The animals performed
 219 a fixation or discrimination task for liquid rewards while vi-
 220 sual stimuli were presented within the receptive field of a
 221 single MT neuron. All surgical and behavioral procedures
 222 conformed to guidelines established by the U.S. Department
 223 of Health and Human Services (National Institutes of Health)
 224 in the *Guide for the Care and Use of Laboratory Animals*
 225 (1996).

226 Behavioral task

227 For the first experiment, two monkeys performed a
 228 simple fixation task while colored gratings were presented
 229 on the monitor. Each trial was initiated by illumination of a
 230 centrally located small black square. The monkey had 2 s to
 231 acquire this fixation point. The stimulus appeared 500 ms
 232 after the monkey began fixating and remained on the screen
 233 for 1 s. After the stimulus disappeared, another 300 ms
 234 passed before the fixation point was extinguished, which
 235 signaled the end of the trial. If the monkey successfully
 236 completed the trial (i.e., maintaining fixation within a 1.0°
 237 electronic window), she was rewarded with a drop of juice
 238 or water at the end of the trial. If the monkey broke fixation
 239 at any point or failed to initiate fixation, the trial was
 240 aborted and no reward was given.

241 For the second experiment, one monkey discriminated
 242 the direction of motion in contrast-varying Gabors (see
 243 [Visual Stimuli](#)). Gabors were used instead of gratings to
 244 eliminate position cues at the edge of the stimulus that the
 245 monkey might use in performing the task. Each trial began
 246 as it did in the fixation task: A fixation point was illumi-
 247 nated, and the monkey had 2 s to initiate fixation. Upon
 248 fixation, 280 ms passed, after which two eccentric targets
 249 appeared, placed along the axis of motion to either side of

the (as yet invisible) stimulus aperture. After another 120
 ms, the stimulus appeared, and remained on the screen for 1
 s. A final fixation interval of 300 ms occurred before the
 fixation point went out, which was the monkey's cue to
 make a saccade to the target that lay in the direction of
 motion that she had perceived. The monkey was given a
 maximum of 800 ms to initiate this saccade; typically,
 saccade initiation time was about 300 ms. After a target
 was acquired, the monkey had to hold fixation on the target
 for another 150 ms before the target was extinguished. At
 this point, a reward was delivered for a correct choice.
 Neither rewards nor any negative reinforcement was given
 on incorrect trials. If the monkey failed to adhere to any of
 the time-interval requirements, either breaking fixation or
 failing to initiate fixation or a saccade in the allotted time,
 the trial was aborted and no reward was given.

Recording methods

We recorded extracellular action potentials from single
 MT neurons using standard laboratory techniques (Britten
 et al., 1992). At the beginning of each recording session, the
 recording chamber was opened, a stainless steel guide tube
 was inserted 1–3 mm past the dura, and a tungsten micro-
 electrode (Fred Haer, Bowdoinham, ME; 1–5 MΩ) was
 advanced into the brain through the guide tube using a
 hydraulic microdrive (Narishige, Tokyo, Japan). We identi-
 fied the MT area by the pattern of gray and white matter
 transitions during descent, by the characteristic physiologi-
 cal properties of MT neurons, and by the topographic orga-
 nization within the MT area. Action potentials from isolated
 neurons were identified using a window discriminator (Bak
 Electronics, Mount Airy, MD). The occurrence time of each
 action potential was recorded (Hays, Richmond, & Optican,
 1982).

Experimental protocol

We searched for and recorded from only direction-
 selective, S-cone responsive neurons. Approximately 95%
 of the MT neurons we encountered were direction-selective
 and highly sensitive to luminance contrast. Of these neu-
 rons, about 75% also responded measurably to S-cone
 stimuli. Of the S-cone responsive neurons, about 90% were
 direction-selective to S-cone motion; the few nondirection-
 selective neurons were not studied further.

Each experimental session began by isolating an MT
 neuron. Upon isolating a neuron, we qualitatively assessed
 receptive field size and location and the neuron's preferred
 direction of motion, speed, and spatial frequency. Based on
 these measurements, we selected the sinusoidal grating
 stimulus parameters that produced the largest response.

For the first experiment, we measured neural responses
 to various combinations of S- and L,M-cone contrast

300 gratings moving in the preferred direction while the mon-
301 key fixated. The various colored stimuli were presented in
302 pseudorandom (interleaved) order within a single block of
303 trials. S-cone contrasts ranged from 0% to 64%, and L, M-
304 cone contrasts ranged from –12% to 12%. Each trial type
305 was repeated a minimum of five times, but more typically
306 eight times. The response rate during the interval before
307 stimulus onset served as a measure of the spontaneous
308 firing rate. Our database for this experiment consists of 42
309 neurons from three hemispheres in two monkeys.

310 For the second experiment, we recorded MT neural
311 activity while the monkey discriminated the direction of
312 motion in S-cone and luminance contrast Gabors moving in
313 the preferred or null direction of the neuron under study.
314 Contrast was varied in log steps to measure contrast
315 threshold. We obtained about 20 repetitions of each trial
316 condition (mean = 21, range = 8–40). S-cone and lumi-
317 nance stimuli were presented in separate blocks because we
318 found that the monkey performed suboptimally on S-cone
319 contrast trials when these stimulus types were interleaved.
320 Different contrast levels were pseudorandomly interleaved
321 within each block. Data are included for which the monkey
322 achieved the following criteria for adequate behavioral
323 performance: (a) at least 90% correct at the highest contrast
324 and (b) a threshold that was good and a slope that was
325 reasonably steep, based on the monkey's routine perfor-
326 mance. Our database consists of 67 neurons from two
327 hemispheres of one monkey. For 47 of these neurons, we
328 were able to obtain data sets for both stimulus types. Our
329 database contains a total of 59 neurons for S-cone contrast
330 and 55 neurons for luminance contrast.

331 Visual stimuli

332 Visual stimuli were presented on a 48-cm CRT monitor
333 (HP910, Hewlett Packard, Palo Alto, CA). The monitor
334 refresh rate was 100 Hz, and a 12-bit/channel graphics card
335 controlled the primary intensities. We determined the
336 relationship between digital value and signal output level
337 for each of the display primaries (gamma correction), and
338 we verified that the signals from the monitor primaries
339 combined additively (Brainard, Pelli, & Robson, 2002) by
340 repeated photometric measurements (J17 photometer, Tek-
341 tronix, Beaverton, OR).

342 The test stimuli consisted of sine-wave gratings for the
343 first experiment and Gabors for the second experiment,
344 windowed with a circular aperture (5–12° diameter).
345 Gabors are sine-wave gratings in which the aperture is
346 Gaussian, such that contrast is maximal at the center and
347 falls off smoothly to effectively zero contrast at the edges.
348 Each stimulus contained a single spatial frequency (0.1–
349 1.0 cycles/deg) drawn from a low range to limit chromatic
350 aberration. Stimuli were presented at a 57-cm viewing
351 distance on an achromatic background (45 cd/m²; $xy =$
352 0.2813, 0.2941, correlated color temperature = 4036 K).

Stimulus speed was selected to elicit robust responses 353
from the neuron under study. The temporal frequency range 354
was 0.7–12 Hz (median = 5.7 Hz). We did not observe any 355
correlation between temporal frequency and the interaction 356
between the L,M- and S-cone signals (coefficient b in 357
Equation 5; see Figure 8). 358

Using radiometric measurements of the phosphor spectra 359
(PR650, Photo Research, Chatsworth, CA) and the color 360
matching functions (Smith & Pokorny, 1972, 1975), we 361
computed the relationship between display primary inten- 362
sities and L-, M-, and S-cone contrast (Wandell, 1995). In 363
addition to making this calculation, we measured the final 364
spectral output of the monitor when displaying these 365
stimuli and back-calculated the delivered cone contrasts 366
to estimate the average error in cone contrast presentation. 367
Nominal S-cone contrast errors were almost always less 368
than 1%, and never more than 5%. Nominal L,M-cone 369
contrast errors were always less than 0.5%. Calibration 370
measurements were repeated every 6 months during the 371
course of the experiments. 372

Macular pigment and chromatic aberration 373

Two important factors, beyond display calibration, in- 374
fluence cone absorptions: spatial variations in macular 375
pigment density and longitudinal chromatic aberration. 376
The macular pigment is an inert spectral filter present at 377
different densities across the visual field. It is present in 378
highest density (0.35) in the central visual field, falling to 379
half density at 2.5° (Bour, Koo, Delori, Apkarian, & 380
Fulton, 2002; Chen, Chang, & Wu, 2001). The pigment 381
appears to be absent beyond 8° of eccentricity (Snodderly, 382
Handelman, & Adler, 1991). The receptive field centers in 383
our experiments ranged from 3.2° to 18.0°, so that most 384
receptive fields spanned regions containing a range of 385
macular pigment densities. 386

To account for the macular pigment, we calculated cone- 387
isolating directions differentially for receptive fields in the 388
central 5° versus those beyond. For neurons with receptive 389
fields within the central 5°, we used the published Smith– 390
Pokorny fundamentals. For neurons with receptive fields 391
outside the central 5° (30/42 neurons, 71%), we corrected 392
the fundamentals by removing a 0.35 macular pigment 393
density (Bone, Landrum, & Cains, 1992; Stockman, 394
Sharpe, & Fach, 1999). In control experiments with human 395
observers, we confirmed that correcting for this difference 396
produced good S-cone isolation. Specifically, with the 397
macular pigment correction, adaptation to a yellow light 398
increased L,M-cone detection thresholds by at least twofold 399
for three human observers while leaving S-cone thresholds 400
virtually unchanged in the periphery (data not shown). 401
Without this correction for macular pigment density, the 402
yellow light influenced estimated S-cone thresholds. 403

In addition, chromatic aberration limits the ability to 404
isolate different cone inputs because the optics transform 405

406 the contrast separately at each wavelength. In particular, at
 407 high spatial frequency, short wavelength signals do not pass
 408 through the optics (Marimont & Wandell, 1994), such that
 409 the retinal image differs from the calibrated display image.
 410 We can substantially allay this concern by restricting the
 411 range of spatial frequencies used to below 1 cycle/deg, a
 412 cutoff below which chromatic aberration is negligible or
 413 absent (Marimont & Wandell, 1994). We were nevertheless
 414 able to present stimuli at the optimal spatial frequency for
 415 each neuron we studied because MT neurons prefer rela-
 416 tively low spatial frequencies (and we verified this for each
 417 neuron we isolated).

418 To better understand the consequences of chromatic
 419 aberration and misestimation of the macular pigment, we
 420 used a simulation of the image formation and cone absorp-
 421 tion processes (Cottaris, 2003; Farrell, Xiao, Catrysse, &
 422 Wandell, 2003). The simulation begins with the spectral
 423 power distribution of the CRT stimuli and simulates the
 424 passage of the light through the human optics (Marimont &
 425 Wandell, 1994) and the capture of the retinal irradiance by
 426 the three types of cone photoreceptors (simulation software
 427 can be downloaded from [http://white.stanford.edu/~brian/
 428 private/JOVAnalysis.htm](http://white.stanford.edu/~brian/private/JOVAnalysis.htm)). Under our experimental condi-
 429 tions, we estimate L-, M-, and S-cone mean absorption rates
 430 to be 8.9×10^7 , 7.8×10^7 , and 1.9×10^3 absorptions per
 431 second, respectively. For a 1-cycle/deg test stimulus, with
 432 complete certainty in the macular pigment density, a nomi-
 433 nal S-cone contrast at the display of 64% produces a retinal
 434 S-cone contrast of 22% and L- and M-cone contrasts on the
 435 order of 0.4%. Hence, at nominal S-cone contrasts that
 436 produce robust responses, for example, 10%, chromatic
 437 aberration error introduces less than 0.07% contrast of
 438 unwanted signals in the L- and M-cone mosaics. Given that,
 439 in our experiments, we used spatial frequencies at or below
 440 1 cycle/deg and that most of the time the preferred spatial
 441 frequency was 0.3–0.5 cycle/deg, we can eliminate chromatic
 442 aberration as a potential source of error in our calibration.

443 Poor estimation of the macular pigment density is a more
 444 severe source of error. Table 1 illustrates the size of the
 445 estimated error for the case where there is no macular
 446 pigment density but where the stimuli are calculated
 447 assuming a range of (incorrect) pigment densities. The
 448 largest error corresponds to no macular pigment and a
 449 stimulus calculation using a density of 0.36. In this case,
 450 a 64% nominal S-cone contrast stimulus produces an un-
 451 wanted M-cone contrast of 3.2%. In practice, an error of
 452 this size is unlikely because the macular pigment density
 453 falls off to one-half maximum (0.18 density) at 2.5° from
 454 the central fovea; the size of the typical MT receptive field
 455 excludes the possibility that the average macular pigment
 456 density is 0.35. However, at a nominal S-cone contrast of
 457 64%, an unwanted L-cone contrast of 1.1%, and an M-cone
 458 contrast of 1.7% is a real worst-case possibility. It is
 459 important to note that this unwanted cone contrast signal
 460 is out of phase with the S-cone signal and thus should
 461 appear as an opponent M-cone signal.

Table 1. Estimated cone contrast errors due to chromatic aberration and misestimated macular pigment density. Estimated retinal contrasts to a nominal S-cone stimulus (64%) with no macular pigment and various assumed densities.

Assumed pigment density	Retinal contrast (%)			
	L cone	M cone	S cone	
None	0.4	0.4	22.0	t1.5
0.09	0.6	1.2	22.4	t1.6
0.18	1.1	1.7	22.1	t1.7
0.36	1.7	3.2	22.0	t1.8

The macular pigment correction accounts for differences
 between the fovea and periphery. If the estimated density is
 systematically wrong, we might expect to observe different
 S-cone contributions to cell responses when comparing
 foveal and peripheral receptive fields. A systematic com-
 parison of the S-cone contributions as a function of eccen-
 tricity revealed no such differences.

Cone isolation control experiment

MT neurons are very sensitive to luminance motion
 contrast (Cheng, Hasegawa, Saleem, & Tanaka, 1994;
 Sclar, Maunsell, & Lennie, 1990); in the conditions used
 here, reliable luminance responses were evoked with stim-
 ulus contrasts of 3% and, for some cells, with contrasts as
 low as 1.5%. Because calibrating a monitor to accurately
 display S-cone-isolating stimuli is notoriously difficult,
 during the first experiment, we performed a control exper-
 iment to verify that responses measured using S-cone-
 isolating stimuli were not, in fact, driven by unwanted L-
 or M-cone contrast. In these control experiments, we added
 a bright yellow light to the background to reduce L- and M-
 cone contrast (Chatterjee & Callaway, 2002; Seidemann et
 al., 1999) and measured neural responses to L,M- and S-
 cone-isolating stimuli in the presence and absence of this
 background.

To create the yellow background light, we mounted
 twelve 75-W halogen lamps in front of the monitor on a
 track-lighting system. A filter that passes only long wave-
 lengths (>550 nm) was placed in the optical path between
 the lights and the display (Wratten 15, Eastman Kodak,
 Rochester, NY). The lamps were arranged so as to create a
 uniform field of illumination on the monitor and were
 positioned close to the monitor such that the luminance
 of the monitor in the presence of the lamps was roughly
 five times higher than the baseline luminance of the mean
 gray background (215 vs. 45 cd/m^2).

We performed this control experiment for 17 cells. Two
 independent contrast series—one S-cone and one L,M-
 cone—were randomly interleaved within a block of trials.
 We collected three such blocks of trials, the first and the
 third under normal illumination and the second under

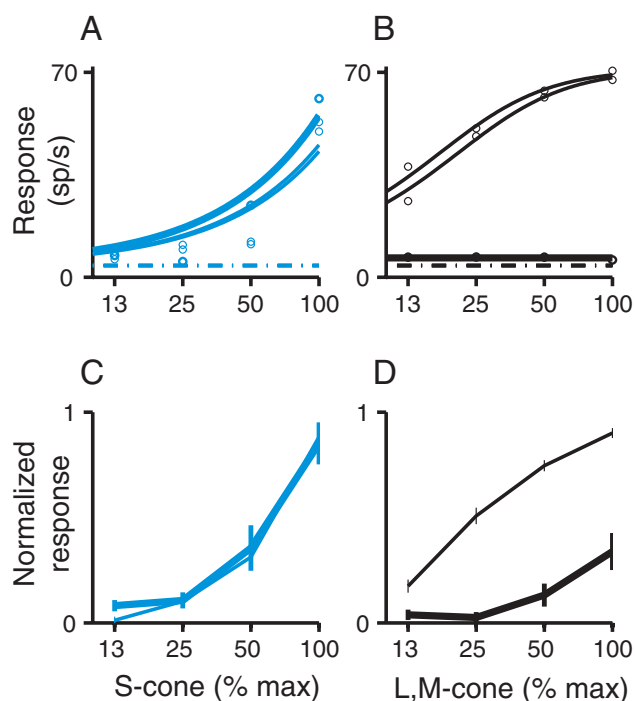


Figure 3. Cone-isolation control experiment. (A) S-cone contrast response functions, plotted against percent maximum contrast, for one neuron obtained before, during, and after adaptation to the yellow light. Heavy line: yellow light condition. Spontaneous firing rate is indicated by the horizontal dotted line. (B) L,M-cone contrast response functions for the same neuron, plotted as in panel A. (C) Population average ($n = 17$) of the normalized S-cone contrast response function, plotted against percent maximum contrast. Heavy line indicates the yellow light condition; the regular line indicates the average response during the pre- and postadaptation conditions. Error bars are standard error of the mean. (D) Population average of the normalized L,M-cone contrast response function, plotted as in panel C. Maximum contrast varied from cell to cell to capture the dynamic range of the neuron's response, varying primarily as a function of receptive field eccentricity. Maximum L,M-cone contrast varied from 5% to 30%; maximum S-cone contrast varied from 40% to 80%. For each neuron, S- and L,M-cone contrast trials were randomly interleaved within a block.

502 yellow light illumination. Between each block, the monkey
503 adapted to the new lighting condition for a minimum of 4
504 min, an interval sufficient to ensure stable retinal contrast
505 adaptation (Perlman & Normann, 1998; Poot, Snippe, &
506 van Hateren, 1997; Yeh, Lee, & Kremers, 1996). The
507 stimuli were tailored to the neuron's tuning properties, just
508 as in the main experiment (see Experimental Protocol).
509 Stationarity of the responses over time is critical for a valid
510 comparison of responses in a block design of this nature;
511 five additional cells were discarded from this analysis
512 because the baseline firing rate varied by more than a
513 factor of two between the first and third (i.e., nonyellow
514 light) control blocks.

515 For S-cone signals, the contrast response function was
516 virtually unchanged in the presence of the yellow back-
517 ground (Figure 3A and 3C), whereas for L,M-cone sig-
518 nals, MT responses were substantially reduced (Figure 3B

and 3D). Figure 3A and 3B show responses from a single
519 MT neuron that exhibited a clear effect of the adapting
520 light. Thick lines represent data obtained from blocks when
521 the yellow light was on. The S-cone response function re-
522 mained nearly constant between the two conditions, whereas
523 the luminance response function was dramatically reduced
524 by the yellow background light. Both signals returned
525 to control levels after removal of the yellow background
526 light.

The average response to the yellow light control for the
528 test population of 17 cells is shown for S- (Figure 3C) and
529 L,M-cone (Figure 3D) stimuli. Heavy lines again depict the
530 yellow-light-adapted condition. Recall that within a partic-
531 ular light adaptation condition, the L,M- and S-cone data
532 were collected on interleaved trials. Although the magni-
533 tude of the effect on L,M-cone responses varied somewhat
534 across cells, the population average, which includes stan-
535 dard error bars, clearly shows a consistent effect of the
536 yellow light on these responses and no significant effect on
537 S-cone responses.

To quantify this effect, for each neuron, the responses
539 were fit with a saturating function, which is the cone-
540 interaction model (Equation 5) reduced to one cone signal:
541

$$r = m \left(\frac{x}{\sqrt{c + x^2}} \right), \quad (6)$$

where x is either an L,M- or an S-cone contrast, c is a
542 saturation constant, and m is a proportionality constant.
543 Maximum response and contrast threshold were extracted
544 from the fitted equation. Maximum response was given by
545 the response magnitude at maximum contrast; threshold
546 was taken as the contrast at which the neural response was
547 halfway between the spontaneous firing rate and the max-
548 imum response.

Yellow light adaptation elevated the L,M-cone thresh-
550 old 2.5-fold, on average, whereas the S-cone threshold
551 remained unchanged; adaptation reduced the L,M-cone
552 maximum response to about 40% of its unadapted value,
553 on average, whereas the S-cone maximum response again
554 remained unchanged (Table 2).

We also considered the possibility that the neural
556 responses may be driven significantly by rod-initiated
557 signals. There are two reasons we think that this is unlikely.
558 First, the mean scotopic luminance in the yellow-light
559

Table 2. Cone-isolation control experiment. Ratio of measures of the mean neural response under the yellow light condition to the response under the normal light condition, computed separately for each neuron. Mean and standard deviation of these ratios are given.

	L,M cone	S cone	
Contrast threshold	2.43 ± 1.35	1.04 ± 0.24	t2.4
Response magnitude	0.36 ± 0.34	1.00 ± 0.54	t2.5

560 condition is 298 cd/m² whereas the monitor alone is 132
 561 cd/m². Hence, the added yellow light reduced any rod
 562 contrast by a factor of two, and this contrast reduction
 563 should have been matched by a sensitivity loss; however, it
 564 was not. Second, from simulations, we estimate the un-
 565 wanted rod contrast caused by the S-cone-isolating stimuli
 566 to be from 1% to 6%. Behavioral increment thresholds
 567 suggest a contrast threshold of 10% over most of the
 568 scotopic range, rising to more than 100% at background
 569 levels comparable with those of the yellow light control
 570 (Aguilar & Stiles, 1954). If behavioral thresholds measure
 571 sensitivity limited by the rods, then the unwanted rod
 572 contrast is too low to influence the MT neural responses.

573 In practice, we were generally unable to maintain single-
 574 cell isolation long enough to collect responses to both the
 575 data set for the first experiment (e.g., Figure 2A) and the
 576 three blocks of the yellow-light control experiment. Thus,
 577 the interaction grids and the yellow light controls were
 578 performed on largely nonoverlapping sets of cells. It seems
 579 safe to assume, however, that the results of the yellow-light
 580 control experiments are applicable to our entire pool of MT
 581 neurons because (a) the results of the yellow light control
 582 were consistent across neurons and (b) the selection crite-
 583 ria, range of tuning properties, and visual stimuli were the
 584 same for the two groups of experiments. We take the results
 585 in Figure 3 as a confirmation that responses to the nomi-
 586 nally S-cone stimulus were indeed driven by S-cone con-
 587 trast, rather than by unwanted L- or M-cone contrast.

588 Data analysis: Experiment 1

589 In the first experiment, we fit each data set with a cone-
 590 interaction model to determine the nature of the cone inter-
 591 actions in the neural response.

592 Cone-interaction model

593 We fit the cone-interaction model (Equation 5) to each
 594 neural data set using a minimum-slope search algorithm
 595 (fminsearch in Matlab). The fit minimized a model error
 596 comprised of the sum of two terms: (a) the sum of squared
 597 errors between the data and the model and (b) the sum of
 598 squared errors between the derivative of the data and the
 599 derivative of the model. The first term requires the model to
 600 fit the data. The second term enforces a certain degree of
 601 smoothness onto the fitted surface. This was necessary
 602 because the five-parameter model at times produced un-
 603 wanted approximations to individual data points. The
 604 derivative was calculated by taking the difference between
 605 neighboring pairs of points on the grid. This was done for
 606 the two cardinal directions (along the x and y axes), but not
 607 along the diagonals.

608 We quantified the goodness-of-fit of the cone-interaction
 609 model using a metric that compares the ability of the model

to predict the data (“model error”) to the ability of the data
 to predict itself (“data error”). We calculated the data error
 by dividing the individual responses to each stimulus
 randomly into two groups, and treating one group as the
 “data” and the other as the “prediction.” We considered
 the sum of squared deviates between the two sets to be the
 data error. Model error was the sum of squared deviates
 between the model, fit to the “data” group data set, and the
 data points derived from the “prediction” group data set.
 (This was done to keep the variability comparable in these
 two error metrics.) A model error that is equal to or less
 than the data error indicates that the model fits the data as
 well as can be expected given the intrinsic variability of the
 data. We devised this metric because we could not find one
 among the standard stock of statistical tests (e.g., chi-
 squared) that dealt adequately with two-dimensional data
 and for which the expected value for a good fit was easily
 determined.

Ninety-five percent confidence intervals for the fitted
 parameters were computed using a bootstrap method
 (resampling each data point with replacement, then refitting
 the cone model) with 500 repetitions.

Data analysis: Experiment 2

In the second experiment, we performed two analyses on
 the simultaneously collected neural and behavioral data.
 The first analysis, the neurometric–psychometric (NP) com-
 parison, allows us to quantify the sensitivity of the neuron
 under study to motion relative to the monkey’s psychophys-
 ical sensitivity to that same motion. The second analysis,
 choice probability (CP), assesses the degree of correlation
 between the trial-to-trial variability in the neural response
 and the monkey’s perceived direction of motion.

Neurometric-psychometric comparison

To assess sensitivity to motion, we measured neural
 responses to S-cone and luminance stimuli at a range of
 contrasts. We obtained psychophysical contrast threshold
 and slope for each contrast series by fitting a sigmoid curve
 to the data set (percent correct as a function of contrast;
 e.g., see Figure 11B). We used a cumulative Weibull
 function, which has the form:

$$p = 1 - 0.5 e^{-\left(\frac{x}{\alpha}\right)^\beta}, \quad (7)$$

where x is the contrast and p is the proportion correct (range =
 0–1). On a logarithmic x axis, the coefficients α and β
 determine the horizontal offset and slope of the curve,
 respectively (Treutwein, 1995). We defined contrast threshold
 as the contrast at which the monkey performed at 75% correct
 (the midpoint between chance and perfect performance).

656 More generally, this psychophysical function has the
657 form:

$$p = s - (s - z) e^{-\left(\frac{z}{\alpha}\right)^\beta}, \quad (8)$$

658 where s is the saturating level of performance (units,
659 proportion correct; range = 0–1) and z is chance perfor-
660 mance level. In 2AFC paradigms, $z = 0.5$. When $s = 1$,
661 Equation 8 reduces to Equation 7. For a few data sets, a
662 better fit was obtained using Equation 8 (with $z = 0.5$ and s
663 allowed to vary), as revealed by a better chi-squared
664 measure of goodness-of-fit. This reflected the fact that in
665 those experiments, maximal performance was somewhat
666 less than 1. In these cases, Equation 8 was used to obtain
667 estimates of α and β .

668 We used a comparable metric, called the *neurometric*
669 *function*, to compute the sensitivity of individual neurons
670 (Britten et al., 1992). In brief, for each stimulus type and
671 contrast, we assessed the ability of an ideal observer to
672 distinguish between preferred and null motion by calculat-
673 ing the receiver operating characteristic (ROC). The ROC
674 curve was constructed by plotting the proportion of pre-
675 ferred motion trials for which the average neural firing rate
676 falls above a criterion value, against the same quantity
677 calculated for null motion trials, for each possible criterion
678 from zero to the maximum observed firing rate. The area
679 under the ROC curve represents the percent of trials in
680 which an ideal observer could correctly identify the direc-
681 tion of motion at this contrast (Green & Swets, 1966). The
682 resulting data set—proportion correct as a function of
683 stimulus contrast—was then fit with a sigmoid function,
684 and the threshold and slope of this function was extracted
685 using the same method as for the psychophysical data
686 (Figure 11B).

687 This analysis gives us the ability to examine the rela-
688 tionship between the two thresholds (or slopes) by calculat-
689 ing their ratio. The neural metric was divided by the
690 psychophysical metric to yield the NP ratio. This quantity
691 was calculated individually for each neuron. The average
692 NP ratio was computed using the geometric mean.

693 Choice probability

694 A neuron's response to a particular stimulus is variable.
695 The behavioral response is also variable for contrasts in the
696 threshold region: On some trials, the monkey guesses
697 correctly, on other trials incorrectly. To assess whether
698 these two variables are correlated on a trial-to-trial basis,
699 we calculated a quantity we refer to as *choice probability*
700 (Britten, Newsome, Shadlen, Celebrini, & Movshon, 1996).

701 The CP calculation uses a metric similar to the NP
702 comparison but compares the distributions of firing rates
703 when the monkey chose one direction of motion versus the
704 other for a single-stimulus condition (e.g., see Figure 12B).

Note that these distributions are distinct from those used in 705
the previous analysis, because they are sorted by behavioral 706
choice rather than by the direction of stimulus motion. This 707
analysis is only possible for stimulus conditions for which 708
the monkey made errors and thus made different choices on 709
different trials. We, therefore, only performed this analysis 710
for conditions in which the monkey made at least three 711
errors. CP is a metric that varies between .5 and 1 and 712
indicates the probability with which we can predict the 713
monkey's choice, given the neural firing rate on a particu- 714
lar trial. When CP = .5, we do no better than chance; when 715
CP = 1, we can predict perfectly the monkey's response. 716

To calculate a single CP value for each neuron, using all 717
of the trials across stimulus conditions, we first normalized 718
the responses within each stimulus condition because 719
different conditions elicited different average levels of 720
firing. To do so, we first converted firing rates on individ- 721
ual trials to z scores, normalized to the average firing rate 722
for that trial condition. 723

724 Results

For the first experiment, we collected data sets from 725
42 cells in two monkeys. S-cone responses were smaller 726
than L,M-cone responses (Figure 4A and 4B), much as 727
Seidemann et al. (1999) observed. A direct comparison of 728
the magnitude of these responses is not possible without 729
converting S- and L,M-cone contrast to a common unit. 730
Accordingly, we selected from our data sets the trial 731
conditions that were purely S- or L,M-cone contrast and 732
plotted the response magnitude as a function of the root- 733
mean-square (RMS) of total cone contrast (Figure 4C). 734
Dividing each measurement of response amplitude by the 735
%RMS cone contrast with which it was elicited yielded a 736
measurement that could be directly compared (Figure 4D). 737
For the cell shown in Figure 4A to 4D, the mean L,M-cone 738
response, in units of spikes per second per unit RMS 739
contrast (response per RMS), was 7.36, whereas the mean 740
S-cone response was 0.66. The response per RMS ratio 741
(S:L,M) was 0.09. 742

Figure 4E displays the distribution of response-per-RMS 743
ratios for the population of neurons in this experiment. The 744
ratios spanned a range, centering on 0.1 (mean = 0.10, $SD =$ 745
0.08), which indicates that MT neural responses to S-cone 746
contrast are, on average, 10% of that to L,M-cone contrast. It 747
may be noted that the response to the low S-cone contrast 748
was sometimes quite small and that the profile of responses 749
to the range of S-cone contrasts was not necessarily linear 750
(e.g., Figure 4C). If small responses represent a neural 751
response that has not yet crossed a threshold of activation, 752
including these values may skew our estimates of the 753
average response to cone contrast. We, therefore, also 754
computed our response-per-RMS ratios using only responses 755

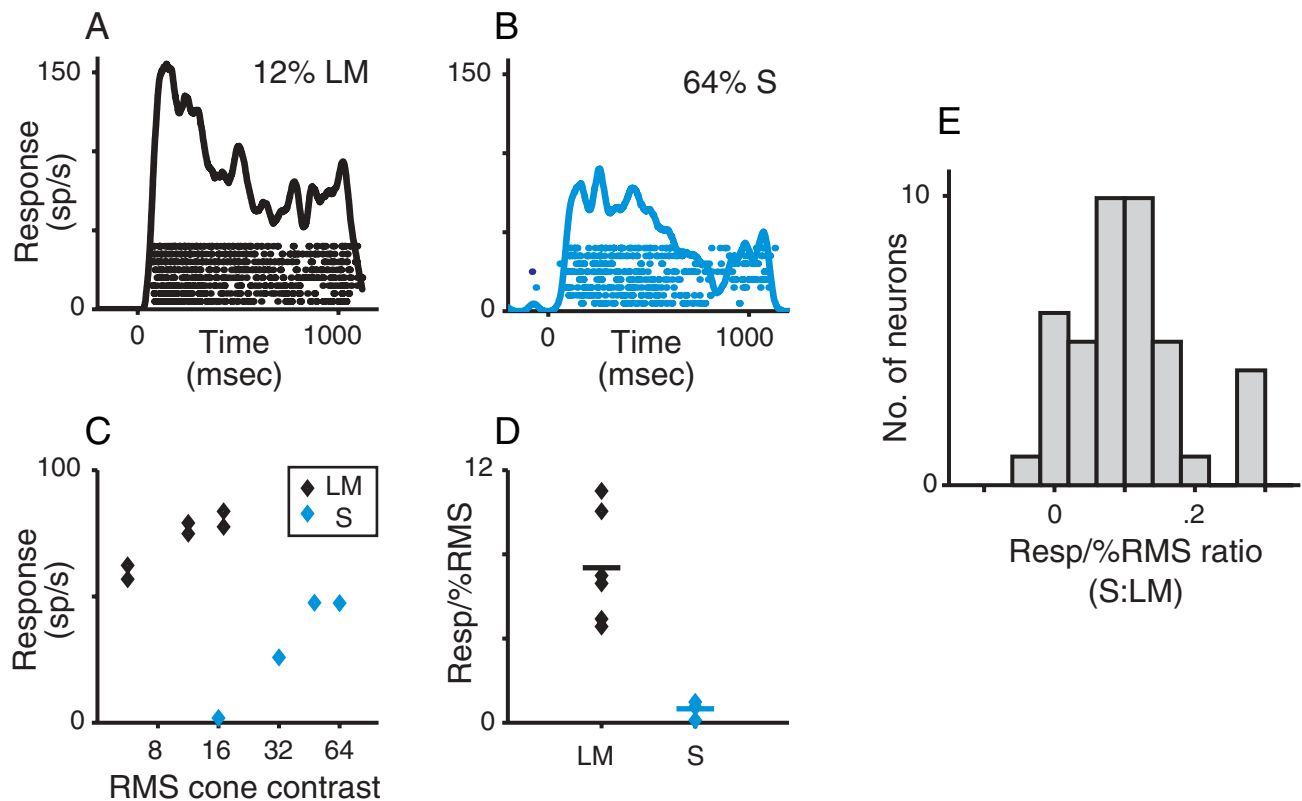


Figure 4. Response magnitude. Relative response magnitude to S- and L,M-cone stimuli. (A). Raster and PSTH for one neuron at 12% L,M-cone contrast. (B). Raster and PSTH for the same neuron at 64% S-cone contrast. (C). Average response (firing rate during stimulus presentation) for the same neuron for several levels of L,M- and S-cone contrast, plotted as a function of RMS cone contrast; each data point represents one stimulus condition. Pairs of points for L,M-cone contrast are for in-phase and out-of-phase stimuli. (D). Response-per-unit RMS for each of the trial conditions shown in panel C. Solid lines mark average response-per-unit RMS. (E). Distribution of the ratio (S:L,M) of average response-per-unit RMS for the 42 neurons in the primary data set.

756 that exceeded 10% of the spontaneous firing rate. The
757 overall result was very similar (mean = 0.11, $SD = 0.07$).

758 The majority of MT neurons in our experiment (69%)
759 were not color-opponent, exhibiting instead some degree of
760 summation of their cone inputs. Figure 2 illustrates a data
761 set obtained from one MT neuron. We collected data sets
762 from 42 cells in two monkeys and observed a range of
763 response profiles. Figure 5 illustrates data sets from three
764 additional neurons, which span the range of response
765 profiles that we observed. The data are displayed as
766 three-dimensional surface plots (Figure 5A, 5C, and 5E)
767 and as slices through constant levels of S-cone contrast
768 (Figure 5B, 5D, and 5F). For the neuron in Figure 5A and
769 5B, the minimum response region fell to the left of the S-
770 cone contrast axis. In contrast, the neuron in Figure 5C and
771 5D yielded minimum responses along the S-cone contrast
772 axis, whereas the neuron in Figure 5E and 5F yielded
773 minimum responses in the right quadrant.

774 Model fits

775 Figure 6 shows the model (Equation 2) fits for each of
776 the neurons shown in Figure 5. The model surfaces capture

the main features of the data. Figure 7 is a scatter plot of the
777 model error against data error for each cell. The model
778 error is equal to or slightly smaller than the data error. The
779 comparison in Figure 7 suggests that the model fits the data
780 well and that further fitting would be beyond the reliability
781 of the data. 782

Analysis of S- and L,M-cone color circuitry

783

The contributions of S- and L,M-cone signals to a
784 neuron's responses can be assessed in several ways. First,
785 note that the two principal terms in Equation 2, one
786 containing an S-cone-initiated signal and the other con-
787 taining only an L,M-cone-initiated signal, combine posi-
788 tively. These two additive terms capture the fact that
789 adding or subtracting L,M- contrast from a fixed S-cone
790 stimulus primarily increases the firing rate (see Theoretical
791 Background). 792

As described in Theoretical Background, the sign of the
793 coefficient b is the critical parameter for evaluating
794 whether the cone interactions show any opponency. This
795 is necessarily the case, because in the model, the only free
796 parameter that can mediate any opponent interaction 797

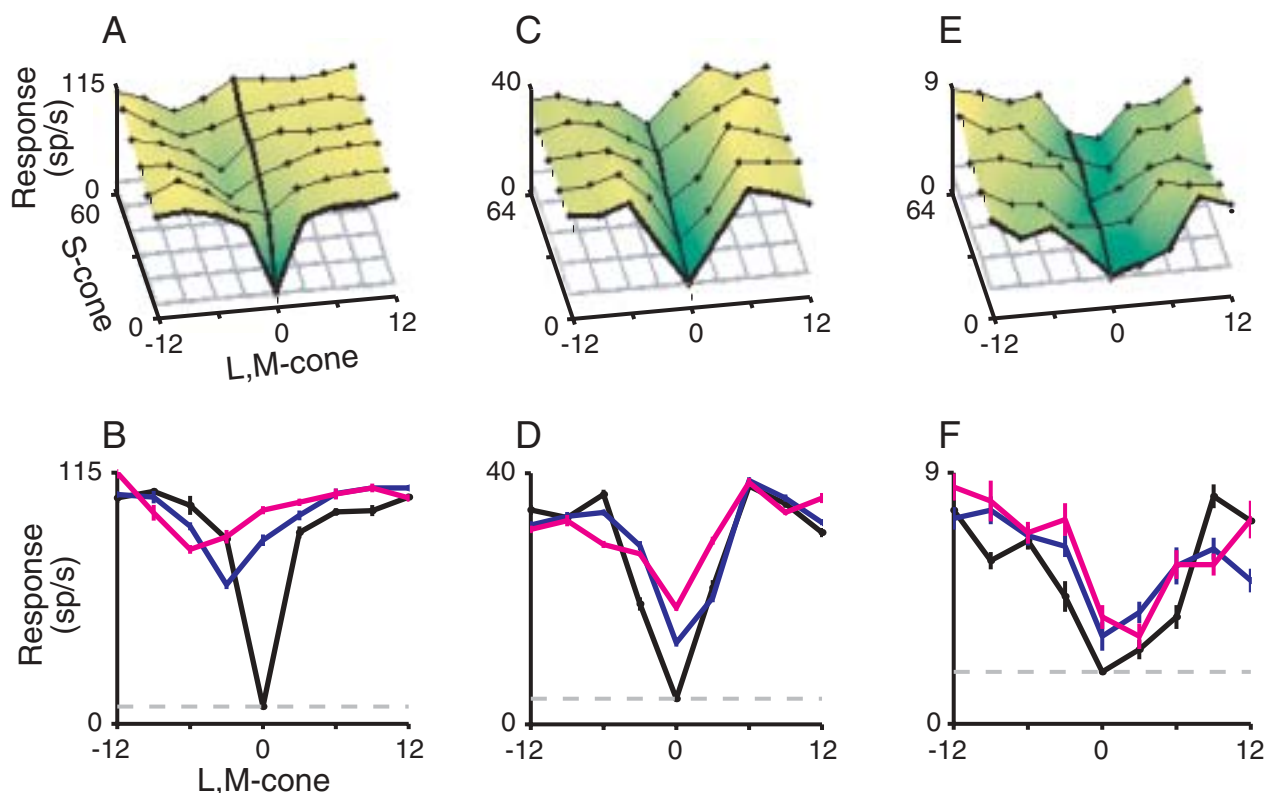


Figure 5. Types of neural response profiles. Three neurons are shown that illustrate the range of response profiles observed. For each cell, two views are displayed, a three-dimensional surface plot, and 3 two-dimensional slices at different S-cone contrast levels. In the surface plots, heavy lines follow the purely S- and L,M-cone contrast response functions, and data points are indicated by black dots. The flat mesh grid in the three-dimensional plots and the dashed line in the two-dimensional slices plots indicate the spontaneous firing rate. The color scale indicates relative response amplitude, running from zero to the maximum firing rate of each cell. (A) and (B). Summation. (C) and (D). Independence. (E) and (F). Opponency.

798 between cone signals before rectification is b . Asymmetries in the neural response profile, which are evident in many of the neurons we recorded (e.g., Figures 2 and 5), must arise from interactions prior to rectification. Figure 8A shows that for the majority of cells, b is higher than zero, indicating summation of S- and L,M-cone signals. However, parameter b is negative for a significant minority of cells, indicating subtraction (i.e., color opponency). The 95% confidence interval for each estimate of b is shown in Figure 8B; few of the confidence intervals include zero. Thus, our sample of MT cells contained units that reliably summed as well as cells that reliably differenced S- and L,M-cone signals.

The magnitude of b measures the relative contribution of the L,M- and S-cone contrasts to the response component represented by the first term. The distribution of the magnitude of b is plotted in Figure 8C separately for positive and negative values. Regardless of whether the cone inputs add or subtract, the magnitude of b centers near a value of 10 (10.26 for additive signals, $b > 0$; 13.55 for differencing signals, $b < 0$).

Figure 9 shows the range of values assumed by the other four parameters in the model, as well as their 95% confidence intervals. Note that although the ranges of param-

eters c_1 and c_2 (Figure 9A and 9B) were quite broad, the confidence intervals were, in general, relatively narrow. Each parameter controls the curvature of the saturating contrast response function for each cone signal, and our neurons exhibited a wide range of profiles, both in terms of degree of curvature, concavity, or convexity and how quickly they saturated. This led to a large range of values for the parameters c_1 and c_2 .

The contribution of S-cone contrast relative to L,M-cone contrast to MT firing rates can also be estimated from the model fits. Because b is relatively small, the S-cone contribution is roughly m_1 ; the L,M-cone contribution is given by $m_1(bl) + m_2$. (Note that this is only an approximation; Equation 5 does not yield a simple term that allows us to compare s and k weightings in terms of all five coefficients.) The ratio of these two quantities, $m_1/(m_1(bl) + m_2)$, is shown for each cell in Figure 10A. The distribution centers on a mean of 0.076, which, interestingly, is comparable to the ratio of S-cone to L- and M-cone photoreceptors in the retina (Curcio et al., 1991; Wandell, 1995).

The values obtained for the parameters of the cone model may give us a hint about the origin of the chromatic responses in the MT area. In Figure 10B, we have plotted

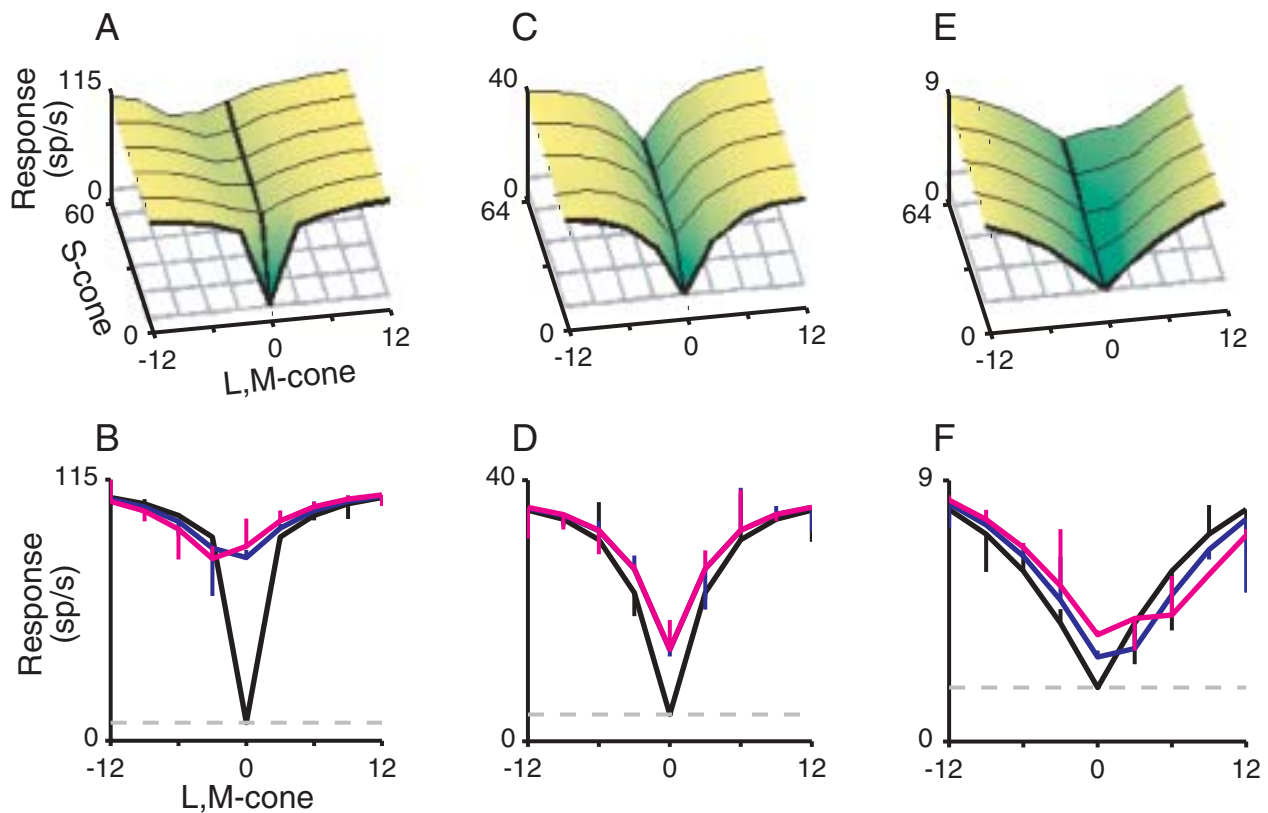


Figure 6. Cone model fits. Cone model fits for each of the neurons shown in Figure 5. Each panel corresponds to the same panel in Figure 5. Vertical bars in two-dimensional slice plots indicate deviation of model from data points. (Note that in panel D, the blue line falls directly behind the magenta line, and so is largely not visible.)

846 the quantity $m_1/(m_1 + m_2)$ against the parameter b . The
 847 parameter b tells us the relative weight of S to L,M within
 848 the term in which they interact, and $m_1/(m_1 + m_2)$ measures
 849 the relative weight of that term with respect to the whole
 850 response. We then note where the different color channels,
 851 measured at the level of the retinal ganglion cells and the
 852 lateral geniculate nucleus (LGN, fall within this plot.
 853 Koniocellular LGN neurons have opposed S- and L,M-
 854 cone inputs, weighted roughly equally (b approximately
 855 -1), and little if any luminance input ($m_1/(m_1 + m_2)$ is
 856 large). Hence, koniocellular neurons fall in the upper center
 857 part of the parameter space, indicated by a small gray
 858 ellipse. We found no cells in the region of the space that
 859 would correspond most closely to koniocellular responses.
 860 Classically described luminance (magnocellular) neurons,
 861 with no S-cone signal (m_1 approximately 0), would fall near
 862 a line at the bottom of this space. (The value of b is
 863 undefined, so all values of b are included.) Magnocellular
 864 neurons with a small S-cone signal, as described by
 865 Chatterjee and Callaway (2002), fall in the region where
 866 b is approximately 10, given the relative weight of cone
 867 signals they observed within those cells (large gray ellipse).
 868 Few of our neurons fall within the “classical” luminance
 869 region, but many fall within the ellipse that describes the
 870 magnocellular data of Chatterjee and Callaway (2002).

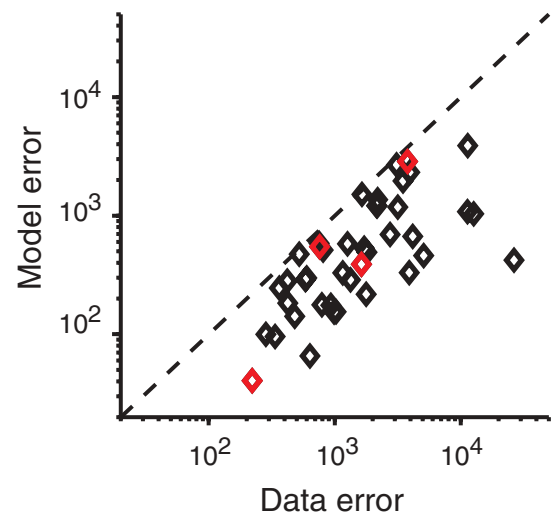
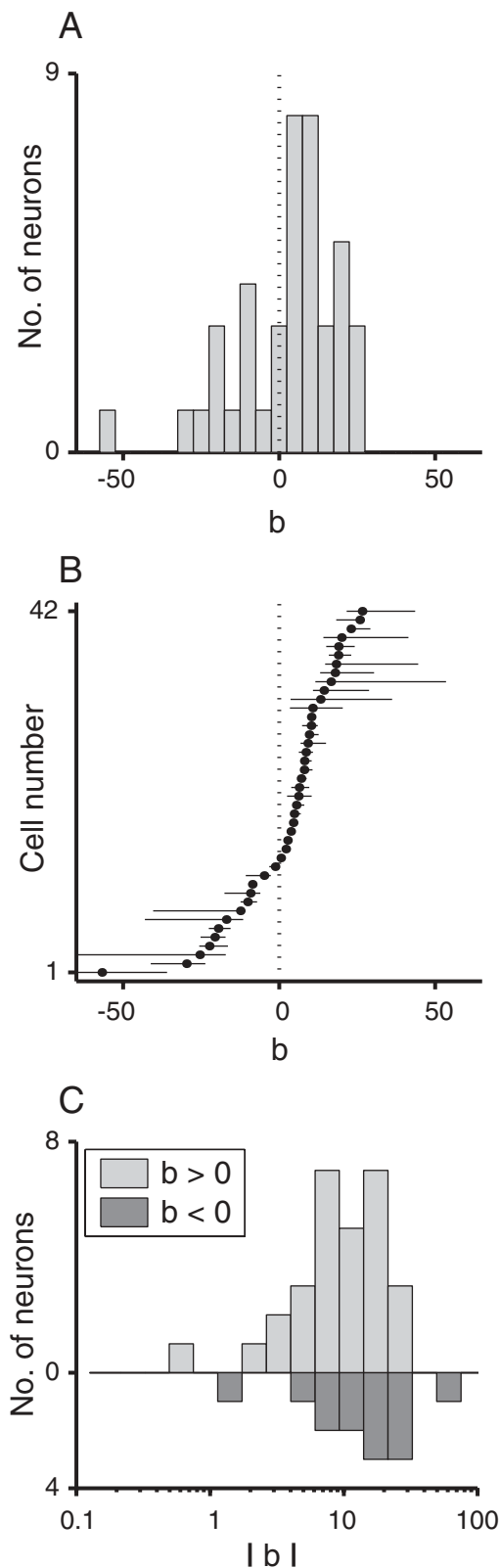


Figure 7. Goodness-of-fit metric for the model fits. The model error, computed as the SSE for the model fit to half of the data, as a function of the data error, computed as the SSE of half of the data to the other half of the data. The solid line is the identity line. Red symbols mark the values for the four neurons shown in Figures 2 and 5.

Neurometric-psychometric comparison

871



For the second experiment, we recorded neural re- 872
sponses while a monkey discriminated the direction of 873
motion in the stimulus. Figure 11A and 11B displays the 874
data obtained from one neuron using S-cone stimuli. The 875
neural response is shown in terms of the average firing rate 876
(Figure 11A) and the neurometric function (Figure 11B) as 877
a function of stimulus contrast. Additionally, Figure 11B 878
depicts the monkey's performance. 879

Both neurometric and psychometric functions varied 880
from experiment to experiment, as did the relationship 881
between them. For the neuron shown in Figure 11A and 882
11B, behavioral sensitivity was slightly higher than neural 883
sensitivity, for both S-cone and luminance contrast (the 884
latter is not shown). To visualize the general relationship 885
between neurons and behavior, we calculated the neuronal 886
and psychophysical threshold for each stimulus (S-cone and 887
luminance) for each cell and compiled distributions of the 888
threshold ratio values (Figure 11C and 11D). The geometric 889
mean of the NP ratio was nearly identical for S-cone and 890
luminance stimuli (threshold = 0.97 and 0.93, respectively), 891
as were the ratios of the slopes of the neurometric and 892
psychometric functions (S-cone slope ratio = 1.02; lumi- 893
nance slope ratio = 1.06). The distributions were not 894
statistically different, either for threshold or for slope. It 895
is reassuring to note that these values are similar to those 896
obtained by Britten et al. (1992), using a different lumi- 897
nance stimulus. 898

Individual MT neurons are apparently carrying motion 899
signals of at least two types: luminance and chrominance. 900
Is the sensitivity of a neuron to luminance motion corre- 901
lated with its sensitivity to chromatic motion? We exam- 902
ined the relationships between S-cone and luminance 903
threshold and between S-cone and luminance slope. Both 904
parameters of the neurometric functions were correlated, 905
threshold more strongly than slope (threshold, $r = .62$, $p < .006$
slope, $r = .32$, $p < .05$). Thus, we see no evidence for 907
separate populations of cells with high sensitivity to only 908
luminance or chromatic stimuli. 909

Choice probability

910

CP quantifies how well the response of the neuron under 911
study predicts the animal's perceptual decisions for a 912

Figure 8. Range and confidence intervals for coefficient b of the model fits. (A). Distribution of coefficient b of the model fits for the population of neurons. Positive values indicate summation; negative values indicate opponency (mean = 6.25, median = 2.22, range = -56.79 to 26.59; mean significantly different from zero; t -test, $p < .001$). (B). Same data as in panel A, where the value and 95% confidence interval of coefficient b are plotted with a point and a line for each cell, ordered by the value of b . (C). Distribution of the magnitude (i.e., the absolute value) of coefficient b , plotted on a log scale (mean for both distributions combined = 10.26, median = 13.55). Coefficients that were positive and negative are plotted in separate histograms, as indicated in the inset.

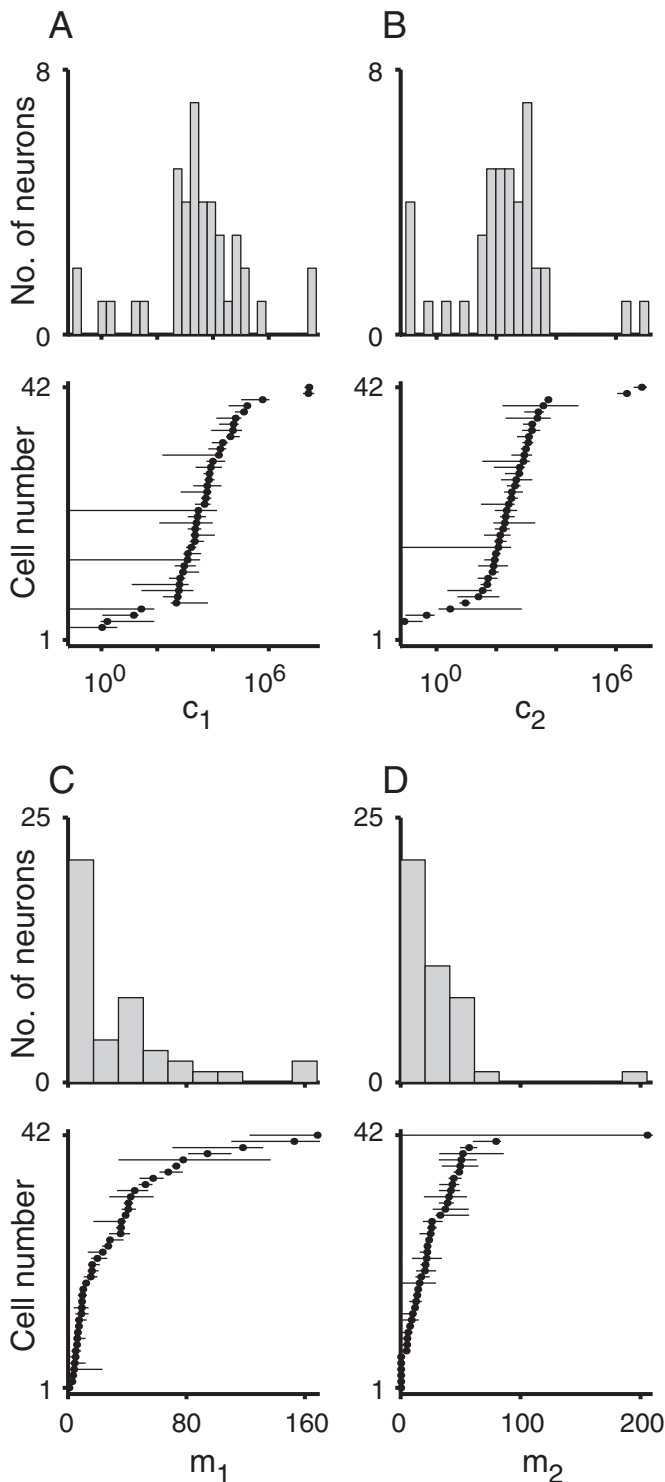


Figure 9. Range and confidence intervals for coefficients of the model fits. (A). Distribution (upper panel) and 95% confidence intervals (lower panel) for coefficient c_1 : mean = 2764, median = 1.29×10^6 , range $<0.01 \times 10^7$ to 2.72×10^7 . (B). Coefficient c_2 : mean = 204.9, median = 2.25×10^5 , range $<.01 \times 10^7$ to 7.16×10^6 . (C). Coefficient m_1 : mean = 17.78, median = 34.09, range = 0.58 to 168.22. (D). Coefficient m_2 : mean = 20.92, median = 27.48, range <0.01 to 205.4.

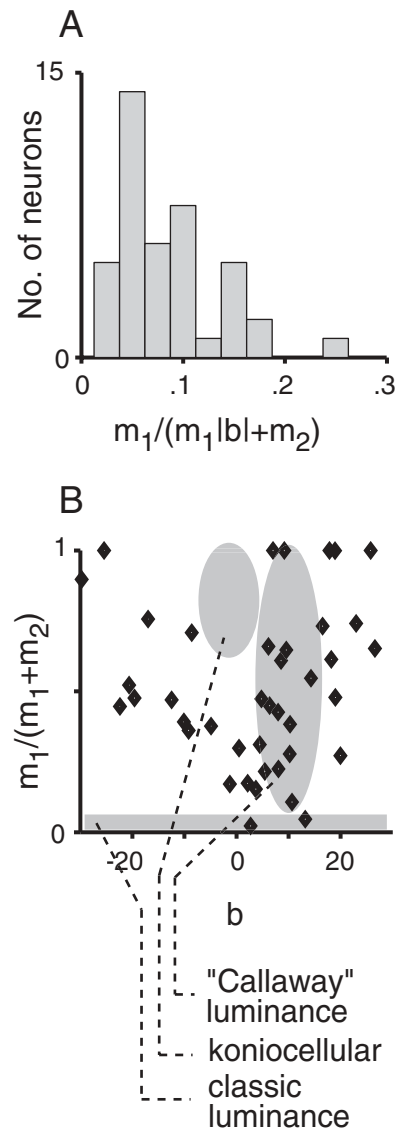


Figure 10. Further analysis of parameters of the model fits. (A). Distribution of the weight of S-cone contrast relative to total L,M-cone contrast in the model fits, captured by the value of $m_1/(m_1|b| + m_2)$. (B). Scatterplot of the relative weight of the first and second terms of the model, captured by the value of $m_1/(m_1 + m_2)$, plotted as a function of coefficient b . Gray ovals indicate regions of this space where neurons in different color pathways would fall (see Results).

single-stimulus condition. [Figure 12A](#) displays a raster and 913 peristimulus histogram (PSTH) of responses to repeated 914 presentation of 4% S-cone contrast moving in the cell’s 915 preferred direction. Trials for which the monkey chose the 916 preferred direction of motion are shown in blue, whereas 917 null-direction choice trials are shown in red. Neural firing 918 rates are variable from trial to trial, and previous studies 919 using random dot stimuli have shown that a higher-than- 920 average firing rate on any individual trial is associated with 921 preferred-direction choices by the monkey. 922

[Figure 12B](#) shows firing rate distributions for preferred- 923 and null-direction choice trials. The blue distribution is 924

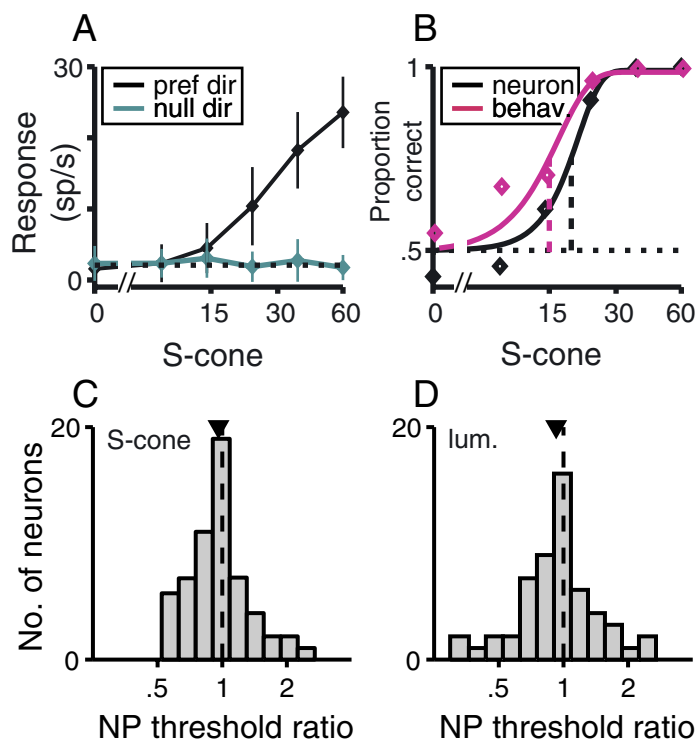


Figure 11. Neurometric–psychometric comparison. (A). Average response (firing rate during stimulus presentation) for one neuron as a function of S-cone contrast, for preferred- and null-direction motion. Error bars denote standard deviation. Dashed line indicates spontaneous firing rate. (B). Neurometric function (black) derived from the data in panel A, with the psychometric function (magenta) for the monkey overlaid. Vertical dashed lines indicate contrast threshold. Horizontal dashed line indicates chance performance level. (C). Distribution of the NP threshold ratio for S-cone contrast stimuli. Black triangle marks average NP ratio across all cells. Vertical dashed line marks a ratio of 1. (D). Distribution of the NP threshold ratio for luminance contrast stimuli. Symbol and dashed line as in panel C.

925 shifted rightward with respect to the red distribution,
 926 indicating that the neuron indeed fired slightly more, on
 927 average, on trials for which the monkey chose the preferred
 928 direction. For the stimulus condition shown in Figure 12A
 929 and 11B, a signal detection analysis yielded a CP of .611
 930 (see Methods). A CP of 1 indicates a perfect correlation
 931 between fluctuations in neural firing rate and behavior,
 932 whereas a CP of .50 indicates that there is no relationship
 933 between the magnitude of the neuron’s response and the
 934 monkey’s choice.

935 A CP can be calculated for any stimulus condition for
 936 which the monkey divides her choices between the two
 937 alternatives. To obtain a single CP for each neuron, we
 938 analyzed all trials for that neuron after converting firing
 939 rates within each contrast level to z scores (see Methods).
 940 Figure 12C displays the CP distributions for all neurons in
 941 this data set for S-cone stimuli, and Figure 12D displays the
 942 same distribution for luminance stimuli. The average CP
 943 for S-cone stimuli was .525, and this mean was signifi-
 944 cantly higher than .5 (t test, $p < .001$). Individual neurons
 945 for which CP was significantly higher than .50 are shaded
 946 (permutation test, $p < .5$).

947 The result for luminance stimuli was very similar (mean
 948 CP = .528, $p < .001$). Britten et al. (1996) obtained a
 949 similar average CP (mean = .548) using a different lumi-

nance stimulus. Most importantly, for our purposes here, 950
 951 the means of the distributions for S-cone and luminance
 952 Gabors were not statistically different ($p > .05$). 952

An important subset of trials to examine is 0% contrast, 953
 954 when no stimulus is actually present on the monitor. Some
 955 artifactual causes of the CP can be ruled out if the CP for
 956 this stimulus condition alone is significant (see the Dis-
 957 cussion section in Britten et al., 1996). CP values for the
 958 0% contrast condition alone were significantly higher than
 959 .5 for both S-cone (CP = .532) and luminance (.520) 959
 960 stimuli, and these distributions were not statistically differ-
 961 ent from each other ($p > .05$). 961

Discussion

962

In the MT area, responses initiated in the S-cones fre- 963
 964 quently sum with responses initiated in the L and M cones. In
 965 a minority of cells, these S-cone signals reliably difference
 966 from L- and M-cone signals (Figure 8A). Thus, both types of
 967 chromatic signals are present in the MT area. In addition,
 968 comparison of simultaneously collected neural and psycho-
 969 physical responses to S-cone and luminance stimuli yields
 970 two results that are consistent with the idea that the MT 970

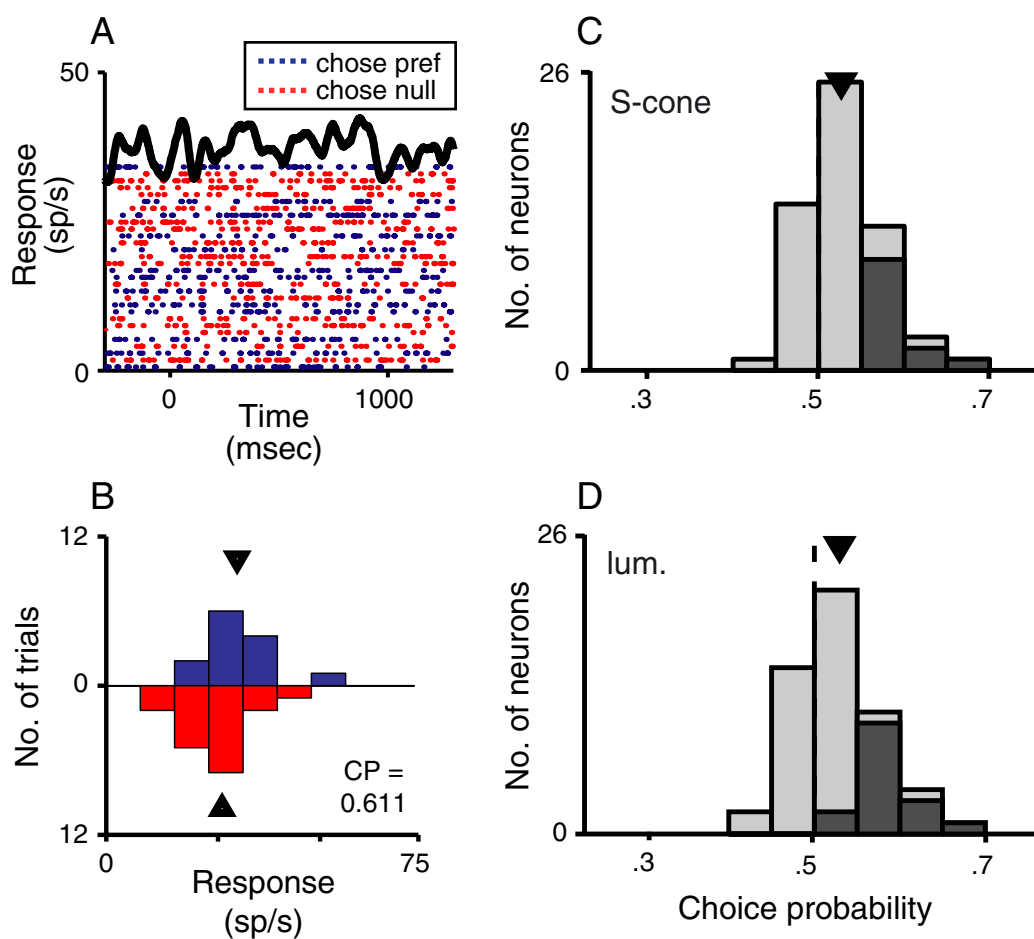


Figure 12. Choice probability. (A). Raster and PSTH for one neuron, for 4% S-cone contrast stimuli moving in the preferred direction. Rows of the raster are color-coded according to whether the monkey chose the preferred (blue) or null (red) direction at the end of the trial. (B). Distributions of average firing rate for the trials shown in panel A, for chose-preferred and chose-null subsets. Black triangles mark the mean of each distribution (blue, 30.60 sp/s; red, 26.33 sp/s). (C). Distribution of the CP value, computed across all trials, for each neuron in the data set, for S-cone contrast stimuli. Black triangle marks the mean of the distribution. Darker shading indicates neurons that were individually significant ($>.5$). (D). Distribution for luminance contrast stimuli. Symbol and shading as in panel C.

971 area could mediate the processing of chromatic motion.
 972 Analysis of neurometric and psychometric thresholds shows
 973 that the relationship between neural and psychophysical
 974 sensitivity is nearly identical for chromatic and luminance
 975 stimuli, despite substantial differences in absolute sensi-
 976 tivity to the two types of stimuli. In addition, significant
 977 choice probabilities of equal magnitude indicate that MT
 978 neural activity is correlated on a trial to trial basis with
 979 psychophysical judgments for both S-cone and luminance
 980 stimuli.

981 **The middle temporal area carries a diverse range** 982 **of chromatic motion responses**

983 Signals from all cone types modulate neural responses in
 984 the MT area. S-cone-initiated signals are weaker, however,
 985 than L- and M-cone-initiated signals (Seidemann et al.,
 986 1999; current study). The variety of chromatic cell types

(Gegenfurtner et al., 1994; Saito et al., 1989; Seidemann 987
 et al., 1999; current study) shows that motion-selective cor- 988
 tex responds to the motion of objects of any color, consistent 989
 with psychophysical measurements (Cavanagh & Anstis, 990
 1991; Chichilnisky, Heeger, & Wandell, 1993; Dougherty, 991
 Press, & Wandell, 1999). It is possible that the diversity of 992
 chromatic cell types simply ensures that motion will be 993
 detected for any color, but that the chromatic information is 994
 not sufficiently organized in the MT area to code the color 995
 of the moving object. In this scenario, the MT area carries 996
 what Albright and colleagues have dubbed “unsigned” 997
 chromatic signals (Dobkins & Albright, 1998; Thiele, 998
 Dobkins, & Albright, 1999). However, the existence of 999
 color-opponent responses in the MT area (Dobkins and 1000
 Albright, 1994; Gegenfurtner et al., 1994; current study) 1001
 raises the possibility that color identity, as well as direction 1002
 of motion, can be decoded from MT responses. Regardless 1003
 of the answer to this question, our results are consistent 1004
 with the idea that chromatic motion is processed by the MT 1005

1006 area (Ffytche, Skidmore, & Zeki, 1995; Thiele et al., 2001)
 1007 as a subclass of all motion stimuli, rather than by, for
 1008 example, visual areas in the ventral stream.

1009 Sources of middle temporal chromatic responses

1010 Our results imply that many S-cone-initiated signals
 1011 arrive in the MT area via a pathway that sums S- and
 1012 L,M-cone signals. One possible source of such a signal is
 1013 the magnocellular pathway, which is known to provide the
 1014 dominant input to the MT area (Maunsell et al., 1990). In
 1015 this regard, our observations correspond with the recent
 1016 findings that S-cone inputs are present in the magnocellular
 1017 layers of the LGN (Chatterjee & Callaway, 2002) and that
 1018 these S-cone inputs sum with the well-known L- and M-cone
 1019 inputs to magnocellular neurons (Chatterjee & Callaway,
 1020 2002). Furthermore, the strength of the S-cone responses
 1021 relative to L,M-cone responses (roughly 1:10) is very sim-
 1022 ilar in the magnocellular LGN (Chatterjee & Callaway,
 1023 2002) and in the MT area (Seidemann et al., 1999; Wandell
 1024 et al., 1999; current study). Alternatively, S-cone signals are
 1025 known to combine in novel ways with L- and M-cone sig-
 1026 nals in V1 (De Valois, Cottaris, Elfar, Mahon, & Wilson,
 1027 2000), and the MT area might simply inherit signals that
 1028 have been mixed at the cortical level.

1029 We also observed color-opponent S-cone responses in a
 1030 significant minority of MT neurons. These signals could, in
 1031 principle, derive from either of two established upstream
 1032 sources: an S-[L,M] signal carried by the large bistratified
 1033 ganglion cells (Chichilnisky & Baylor, 1999; Dacey & Lee,
 1034 1994; Martin, White, Goodchild, Wilder, & Sefton, 1997)
 1035 or an S-off parvocellular cell type (Klug, Herr, Ngo,
 1036 Sterling, & Schein, 2003). The MT area receives a modest
 1037 input from the parvocellular pathway via V1 (Maunsell et
 1038 al., 1990). In addition, a direct projection to the MT area
 1039 from the koniocellular layers of the LGN has recently been
 1040 identified (Sincich, Park, Wohlgenuth, & Horton, 2004).
 1041 However, the responses of the MT color-opponent cells
 1042 were fit best by a model in which the ratio of S- to L,M-
 1043 cone responsivities was roughly 1–10 (see Figure 10B),
 1044 which differs significantly from the roughly equal S- and
 1045 L,M-cone weights described in both the small, bistratified
 1046 ganglion cells of the retina and in the koniocellular layers
 1047 of the LGN (Derrington, Krauskopf, & Lennie, 1984). We
 1048 are not sure how to account for this discrepancy.

1049 Chromatic and luminance motion are processed 1050 similarly in the middle temporal area

1051 The MT area has been shown to play a central role in the
 1052 processing of luminance motion (Newsome & Paré, 1988;
 1053 Salzman, Britten, & Newsome, 1990; Salzman, Murasugi,
 1054 Britten, & Newsome, 1992). If the MT area encodes motion
 1055 from a broader range of visual cues for the purposes of
 1056 motion perception, we would expect to observe the same
 1057 relationships between neuronal activity and psychophysical

performance for different types of motion stimuli. If, on the
 other hand, another brain area performs the perceptually
 relevant processing of chromatic motion signals, we might
 expect to observe substantial differences in the relationship
 between MT activity and performance for S-cone motion
 stimuli. In fact, we found that chromatic motion responses
 in the MT area bear the same signature in relation to
 psychophysical performance as do luminance motion
 responses, including thresholds and slopes of the psycho/
 neurometric functions, and CP. These data support the
 notion that the MT area mediates the perception of motion
 carried by a range of visual cues.

Presuming that the MT area plays an important role in
 processing the motion of chromatic stimuli, it is interesting
 to ask whether the single cells respond to both luminance and
 chromatic motion stimuli, giving rise to cue-invariant
 motion signals (Albright, 1992; O'Keefe & Movshon,
 1998; Stoner & Albright, 1992) or whether different sub-
 populations of MT neurons are dedicated to different types
 of motion. The fact that neuronal thresholds for the two
 types of motion were correlated argues in favor of the
 former idea.

1080 Conclusion

In this article, we have provided the first detailed
 quantitative model of the responses of MT neurons to
 chromatic and luminance stimuli, and we have shown that
 the relationship between MT activity and psychophysical
 performance on a direction discrimination task is indistin-
 guishable for the two types of stimuli. Our data lend weight
 to the hypothesis that MT processes perceptually relevant
 motion signals for all types of stimuli, including chromatic
 ones. A definitive test of this idea will probably require
 inactivation studies of the kind that first demonstrated a
 functional role for the MT area in the perception of
 luminance-defined motion (Newsome & Paré, 1988).

Acknowledgments

This work was supported by the National Eye Institute
 (EY-05603 to W.T.N. and EY-03164 to B.A.W.) and by the
 Howard Hughes Medical Institute (W.T.N. is an HHMI
 investigator). C. L. Barberini and M. R. Cohen were sup-
 ported by HHMI Predoctoral Fellowships. We thank
 Jessica Powell and Stacy Rosenbaum for excellent techni-
 cal assistance. We also thank Greg Horwitz and Robert
 Dougherty for helpful suggestions during editing of the
 manuscript.

Commercial relationships: none.

Corresponding author: Crista L. Barberini

Address: 2236 8th Street, Berkeley, CA 94710

Email: crista@stanfordalumni.org

References

- 1107
- 1108 Aguilar, M., & Stiles, W. S. (1954). Saturation of the rod mechanism of
1109 the retina at high levels of stimulation. *Journal of Modern Optics*, *1*,
1110 59–65. [Article]
- 1111 Albright, T. D. (1992). Form-cue invariant motion processing in
1112 primate visual cortex. *Science*, *255*, 1141–1143. [PubMed]
- 1113 Bone, R. A., Landrum, J. T., & Cains, A. (1992). Optical density
1114 spectra of the macular pigment in vivo and in vitro. *Vision Research*,
1115 *32*, 105–110. [PubMed]
- 1116 Bour, L. J., Koo, L., Delori, F. C., Apkarian, P., & Fulton, A. B.
1117 (2002). Fundus photography for measurement of macular pigment
1118 density distribution in children. *Investigative Ophthalmology and*
1119 *Visual Science*, *43*, 1450–1455, [http://www.iovs.org/cgi/content/full/](http://www.iovs.org/cgi/content/full/43/5/1450)
1120 [43/5/1450](http://www.iovs.org/cgi/content/full/43/5/1450). [PubMed] [Article]
- 1121 Brainard, D. H., Pelli, D. G., & Robson, T. (2002). Display
1122 characterization. In J. Hornak (Ed.), *The encyclopedia of imaging*
1123 *science and technology* (pp. 172–188). Indianapolis, IN: Wiley.
- 1124 Britten, K. H., Newsome, W. T., Shadlen, M. N., Celebrini, S., &
1125 Movshon, J. A. (1996). A relationship between behavioral choice
1126 and the visual responses of neurons in macaque MT. *Visual*
1127 *Neuroscience*, *13*, 87–100. [PubMed]
- 1128 Britten, K. H., Shadlen, M. N., Newsome, W. T., & Movshon, J. A.
1129 (1992). The analysis of visual motion: A comparison of neuronal
1130 and psychophysical performance. *Journal of Neuroscience*, *12*,
1131 4745–4765, <http://www.jneurosci.org/cgi/reprint/12/12/4745>.
1132 [PubMed] [Article]
- 1133 Carandini, M., Heeger, D. J., & Movshon, J. A. (1997). Linearity and
1134 normalization of simple cells of the macaque primary visual cortex.
1135 *Journal of Neuroscience*, *17*, 8621–8644, [http://www.jneurosci.org/](http://www.jneurosci.org/cgi/content/full/17/21/8621)
1136 [cgi/content/full/17/21/8621](http://www.jneurosci.org/cgi/content/full/17/21/8621). [PubMed] [Article]
- 1137 Cavanagh, P., & Anstis, S. (1991). The contribution of color to motion
1138 in normal and color-deficient observers. *Vision Research*, *31*, 2109–
1139 2148. [PubMed]
- 1140 Chatterjee S., & Callaway, E. M. (2002). S-cone contributions to the
1141 magnocellular visual pathway in macaque monkey. *Neuron*, *35*,
1142 1135–1146, [http://www.neuron.org/content/article/fulltext?uid=](http://www.neuron.org/content/article/fulltext?uid=PIIS0896627302008747)
1143 [PIIS0896627302008747](http://www.neuron.org/content/article/fulltext?uid=PIIS0896627302008747). [PubMed] [Article]
- 1144 Chawla, D., Phillips, J., Buechel, C., Edwards, R., & Friston, K. J.
1145 (1998). Speed-dependent motion-sensitive responses in V5: An
1146 fMRI study. *NeuroImage*, *7*, 86–96, [http://www.ingentaconnect.](http://www.ingentaconnect.com/content/ap/ni/1998/00000007/00000002/art00319)
1147 [com/content/ap/ni/1998/00000007/00000002/art00319](http://www.ingentaconnect.com/content/ap/ni/1998/00000007/00000002/art00319). [PubMed]
1148 [Article]
- 1149 Chen, S. F., Chang, Y., & Wu, J. C. (2001). The spatial distribution
1150 of macular pigment in humans. *Current Eye Research*, *23*, 422–434,
1151 [http://www.szp.swets.nl/szp/frameset.htm?url=%2Fszp](http://www.szp.swets.nl/szp/frameset.htm?url=%2Fszp%2Fjournals%2Fce.htm)
1152 [%2Fjournals%2Fce.htm](http://www.szp.swets.nl/szp/frameset.htm?url=%2Fszp%2Fjournals%2Fce.htm). [PubMed] [Article]
- 1153 Cheng, K., Hasegawa, T., Saleem, K. S., & Tanaka, K. (1994).
1154 Comparison of neuronal selectivity for stimulus speed, length, and
1155 contrast in the prestriate visual cortical areas V4 and MT of the
1156 macaque monkey. *Journal of Neurophysiology*, *71*, 2269–2280,
1157 <http://jn.physiology.org/cgi/reprint/71/6/2269>. [PubMed] [Article]
- 1158 Chichilnisky, E. J., & Baylor, D. A. (1999). Receptive-field micro-
1159 structure of blue-yellow ganglion cells in primate retina. *Nature*
1160 *Neuroscience*, *2*, 889–893, [http://www.nature.com/cgi-taf/DynaPage.](http://www.nature.com/cgi-taf/DynaPage.taf?file=/neuro/journal/v2/n10/full/nn1099_889.html)
1161 [taf?file=/neuro/journal/v2/n10/full/nn1099_889.html](http://www.nature.com/cgi-taf/DynaPage.taf?file=/neuro/journal/v2/n10/full/nn1099_889.html). [PubMed]
1162 [Article]
- 1163 Chichilnisky, E. J., Heeger, D., & Wandell, B. A. (1993). Functional
1164 segregation of color and motion perception examined in motion
1165 nulling. *Vision Research*, *33*, 2113–2125, doi:10.1016/0042-
1166 6989(93)90010-T. [PubMed] [Article]
- 1167 Cottaris, N. (2003). Artifacts in spatiochromatic stimuli due to
1168 variations in preretinal absorption and axial chromatic aberration:
1169 Implications for color physiology. *Journal of the Optical Society of*
1170 *America A*, *20*, 1694–1713, [http://josaa.osa.org/abstract.cfm?id=](http://josaa.osa.org/abstract.cfm?id=74133)
1171 [74133](http://josaa.osa.org/abstract.cfm?id=74133). [PubMed] [Article]
- Curcio, C. A., Allen, K. A., Sloan, K. R., Lerea, C. L., Hurley, J. B., 1172
Klock, I. B., et al. (1991). Distribution and morphology of human 1173
cone photoreceptors stained with anti-blue opsin. *Journal of* 1174
Comparative Neurology, *312*, 610–624. [PubMed] 1175
- Dacey, D. M., & Lee, B. B. (1994). The “blue-on” opponent pathway 1176
in primate retina originates from a distinct bistratified ganglion cell 1177
type. *Nature*, *367*, 731–735, [http://www.nature.com/cgi-taf/](http://www.nature.com/cgi-taf/DynaPage.taf?file=/nature/journal/v367/n6465/full/367731a0.html) 1178
[DynaPage.taf?file=/nature/journal/v367/n6465/full/](http://www.nature.com/cgi-taf/DynaPage.taf?file=/nature/journal/v367/n6465/full/367731a0.html) 1179
[367731a0.html](http://www.nature.com/cgi-taf/DynaPage.taf?file=/nature/journal/v367/n6465/full/367731a0.html). [PubMed] [Article] 1180
- Derrington, A. M., Krauskopf, J., & Lennie, P. (1984). Chromatic 1181
mechanisms in lateral geniculate nucleus. *Journal of Physiology*, *357*, 1182
241–265. [PubMed] 1183
- De Valois, R. L., Cottaris, N. P., Elfar, S. D., Mahon, L. E., & Wilson, 1184
J. A. (2000). Some transformations of color information from 1185
lateral geniculate nucleus to striate cortex. *Proceedings of the* 1186
National Academy of Sciences, U. S. A., *97*, 4997–5002, [http://](http://www.pnas.org/cgi/content/full/97/9/4997) 1187
www.pnas.org/cgi/content/full/97/9/4997. [PubMed] [Article] 1188
- Dobkins, K. R., & Albright, T. D. (1994). What happens if it changes 1189
color when it moves?: The nature of chromatic input to macaque 1190
visual area MT, <http://www.jneurosci.org/cgi/reprint/14/8/4854>. 1191
Journal of Neuroscience, *14*, 4854–4870. [PubMed] [Article] 1192
- Dobkins, K. R., & Albright, T. D. (1998). The influence of chromatic 1193
information on visual motion processing in the primate visual 1194
system. In T. Watanabe (Ed.), *High-level motion processing:* 1195
Computational, neurobiological, and psychophysical perspectives (pp. 1196
53–94). Cambridge, MA: MIT Press. 1197
- Dougherty, R. F., Press, W. A., & Wandell, B. A. (1999). Perceived 1198
speed of colored stimuli. *Neuron*, *24*, 893–899, [http://www.neuron.](http://www.neuron.org/content/article/fulltext?uid=PIIS0896627399440366) 1199
[org/content/article/fulltext?uid=PIIS0896627399440366](http://www.neuron.org/content/article/fulltext?uid=PIIS0896627399440366). 1200
[PubMed] [Article] 1201
- Evarts, E. V. (1968). A technique for recording activity of subcortical 1202
neurons in moving animals. *Electroencephalography and Clinical* 1203
Neurophysiology, *24*, 83–86. [PubMed] 1204
- Farrell, J. E., Xiao, F., Catrysse, P. B., & Wandell, B. A. (2003). A 1205
simulation tool for evaluating digital camera image quality. 1206
Proceedings of the SPIE Electronic Imaging Conference, *5294*, 124. 1207
- Ffytche, D. H., Skidmore, B. D., & Zeki, S. (1995). Motion-from-hue 1208
activates area V5 of human visual cortex. *Proceedings of the Royal* 1209
Society of London. Series B, *260*, 353–358. [PubMed] 1210
- Gegenfurtner, K. R., Kiper, D. C., Beusmans, J. M. H., Carandini, M., 1211
Zaidi, Q., & Movshon, J. A. (1994). Chromatic properties of 1212
neurons in macaque MT. *Visual Neuroscience*, *11*, 455–466. 1213
[PubMed] 1214
- Green, D. M., & Swets, J. A. (1966). *Signal detection theory and* 1215
psychophysics. New York: Wiley. 1216
- Hays, A. V., Richmond, B. J., & Optican, L. M. (1982). A UNIX- 1217
based multiple process system for real-time data acquisition and 1218
control. *WESCON Conference Proceedings*, *2*, 1–10. 1219
- Judge, S. J., Richmond, B. J., & Chu, F. C. (1980). Implantation of 1220
magnetic search coils for measurement of eye position: An 1221
improved method. *Vision Research*, *20*, 535–538. [PubMed] 1222
- Klug, K., Herr, S., Ngo, I. T., Sterling, P., & Schein, S. (2003). 1223
Macaque retina contains an S-cone OFF midget pathway. *Journal* 1224
of Neuroscience, *23*, 9881–9887, [http://www.jneurosci.org/cgi/](http://www.jneurosci.org/cgi/content/full/23/30/9881) 1225
[content/full/23/30/9881](http://www.jneurosci.org/cgi/content/full/23/30/9881). [PubMed] [Article] 1226
- Livingstone, M. S., & Hubel, D. H. (1987). Psychophysical evidence 1227
for separate channels for the perception of form, color, movement, 1228
and depth. *Journal of Neuroscience*, *7*, 3416–3468, [http://](http://www.jneurosci.org/cgi/reprint/7/11/3416) 1229
www.jneurosci.org/cgi/reprint/7/11/3416. [PubMed] [Article] 1230
- Marimont, D. H., & Wandell, B. A. (1994). Matching color images: 1231
The effects of axial chromatic aberration. *Journal of the Optical* 1232
Society of America A, *11*, 3113–3122, [http://josaa.osa.org/](http://josaa.osa.org/abstract.cfm?id=882) 1233
[abstract.cfm?id=882](http://josaa.osa.org/abstract.cfm?id=882). [Article] 1234
- Martin, P. R., White, A. J., Goodchild, A. K., Wilder, H. D., & Sefton, 1235
A. E. (1997). Evidence that blue-on cells are part of the third 1236
geniculocortical pathway in primates. *European Journal of Neuro-* 1237
science, *9*, 1536–1541. [PubMed] 1238

- 1239 Maunsell, J. H., & Newsome, W. T. (1987). Visual processing in
1240 monkey extrastriate cortex. *Annual Review of Neuroscience*, *10*, 363–
1241 401, [http://arjournals.annualreviews.org/doi/abs/10.1146/annurev.
1242 ne.10.030187.002051](http://arjournals.annualreviews.org/doi/abs/10.1146/annurev.ne.10.030187.002051). [PubMed] [Article]
- 1243 Maunsell, J. H., & Van Essen, D. C. (1983). Functional properties of
1244 neurons in middle temporal visual area of the macaque monkey. I.
1245 Selectivity for stimulus direction, speed and orientation. *Journal of*
1246 *Neurophysiology*, *49*, 1127–1147, [http://jn.physiology.org/cgi/
1247 reprint/49/5/1127](http://jn.physiology.org/cgi/reprint/49/5/1127). [PubMed] [Article]
- 1248 Maunsell, J. H. R., Nealey, T. A., & DePriest, D. D. (1990).
1249 Magnocellular and parvocellular contributions to responses in the
1250 middle temporal visual area (MT) of the macaque monkey. *Journal*
1251 *of Neuroscience*, *10*, 3323–3334, [http://www.jneurosci.org/cgi/
1252 reprint/10/10/3323](http://www.jneurosci.org/cgi/reprint/10/10/3323). [PubMed] [Article]
- 1253 Newsome, W. T., & Paré, E. B. (1988). A selective impairment of
1254 motion perception following lesions of the middle temporal visual
1255 area (MT). *Journal of Neuroscience*, *8*, 2201–2211, [http://www.
1256 jneurosci.org/cgi/reprint/8/6/2201](http://www.jneurosci.org/cgi/reprint/8/6/2201). [PubMed] [Article]
- 1257 O'Keefe, L. P., & Movshon, J. A. (1998). Processing of first- and
1258 second-order motion signals by neurons in area MT of the macaque
1259 monkey. *Visual Neuroscience*, *15*, 305–317. [PubMed]
- 1260 Perlman, I., & Normann, R. A. (1998). Light adaptation and
1261 sensitivity controlling mechanisms in vertebrate photoreceptors.
1262 *Progress in Retina and Eye Research*, *17*, 523–563, doi:10.1016/
1263 S1350-9462(98)00005-6. [PubMed] [Article]
- 1264 Poot, L., Snippe, H. P., & van Hateren, J. H. (1997). Dynamics of
1265 adaptation at high luminances: Adaptation is faster after luminance
1266 decrements than after luminance increments. *Journal of the Optical*
1267 *Society of America A*, *14*, 2499–2508, [http://josaa.osa.org/abstract.
1268 cfm?id=1958](http://josaa.osa.org/abstract.cfm?id=1958). [PubMed] [Article]
- 1269 Saito, H., Tanaka, K., Isono, H., Yasuda, M., & Mikami, A. (1989).
1270 Directionally selective response of cells in the middle temporal area
1271 (MT) of the macaque monkey to the movement of equiluminous
1272 opponent color stimuli. *Experimental Brain Research*, *75*, 1–14.
1273 [PubMed]
- 1274 Salzman, C. D., Britten, K. H., & Newsome, W. T. (1990). Cortical
1275 microstimulation influences perceptual judgments of motion
1276 direction. *Nature*, *346*, 174–177, [http://www.nature.com/cgi-taf/
1277 DynaPage.taf?file=/nature/journal/v346/n6280/full/346174a0.
1278 html](http://www.nature.com/cgi-taf/DynaPage.taf?file=/nature/journal/v346/n6280/full/346174a0.html). [PubMed] [Article]
- 1279 Salzman, C. D., Murasugi, C. M., Britten, K. H., & Newsome, W. T.
1280 (1992). Microstimulation in visual area MT: Effects on direction
1281 discrimination performance. *Journal of Neuroscience*, *12*, 2331–
1282 2355, <http://www.jneurosci.org/cgi/reprint/12/6/2331>. [PubMed]
1283 [Article]
- 1284 Sclar, G., Maunsell, J. H., & Lennie, P. (1990). Coding of image
1285 contrast in central visual pathways of the macaque monkey. *Vision*
1286 *Research*, *30*, 1–10. [PubMed]
- 1287 Seidemann, E., Poirson, A. B., Wandell, B. A., & Newsome, W. T.
1288 (1999). Color signals in area MT of the macaque monkey. *Neuron*,
1289 *24*, 911–917, [http://www.neuron.org/content/article/fulltext?uid=
1290 PIIS089662739944038X](http://www.neuron.org/content/article/fulltext?uid=PIIS089662739944038X). [PubMed] [Article]
- 1291 Simoncelli, E. P., & Heeger, D. J. (1998). A model of neuronal
1292 responses in visual area MT. *Vision Research*, *38*, 743–761,
1293 doi:10.1016/S0042-6989(97)00183-1. [PubMed] [Article]
- 1294 Sincich, L. C., Park, K. F., Wohlgenuth, M. J., & Horton, J. C. (2004).
1295 Bypassing V1: A direct geniculate input to area MT. *Nature Neuro-*
1296 *science*, *7*, 1123–1128, [http://www.nature.com/cgi-taf/DynaPage.
1297 taf?file=/neuro/journal/v7/n10/abs/nn1318.html&dynoptions=
1298 doi112029204](http://www.nature.com/cgi-taf/DynaPage.taf?file=/neuro/journal/v7/n10/abs/nn1318.html&dynoptions=doi112029204). [PubMed] [Article]
- Smith, V. C., & Pokorny, J. (1972). Spectral sensitivity of color-blind
1299 observers and the cone photopigments. *Vision Research*, *12*, 2059–
1300 2071. [PubMed] 1301
- Smith, V. C., & Pokorny, J. (1975). Spectral sensitivity of the foveal
1302 cone photopigments between 400 and 500 nm. *Vision Research*, *15*, 1303
1304 161–171. [PubMed]
- Snodderly, D. M., Handelman, G. J., & Adler, A. J. (1991).
1305 Distribution of individual macular pigment carotenoids in central
1306 retina of macaque and squirrel monkeys. *Investigative Ophthalmol-*
1307 *ogy and Visual Science*, *32*, 268–279, [http://www.iovs.org/cgi/
1308 content/abstract/32/2/268](http://www.iovs.org/cgi/content/abstract/32/2/268). [PubMed] [Article] 1309
- Stockman, A., Sharpe, L. T., & Fach, C. C. (1999). The spectral
1310 sensitivity of the human short-wavelength cones derived from
1311 thresholds and color matches. *Vision Research*, *39*, 2901–2927,
1312 doi:10.1016/S0042-6989(98)00225-9. [PubMed] [Article] 1313
- Stoner, G. R., & Albright, T. D. (1992). Neural correlates of
1314 perceptual motion coherence. *Nature*, *358*, 412–414, [http://
1315 www.nature.com/cgi-taf/DynaPage.taf?file=/nature/journal/v358/
1316 n6385/abs/358412a0.html&dynoptions=doi1101315821](http://www.nature.com/cgi-taf/DynaPage.taf?file=/nature/journal/v358/n6385/abs/358412a0.html&dynoptions=doi1101315821). [PubMed] 1317
- [Article] 1318
- Thiele, A., Dobkins, K. R., & Albright, T. D. (1999). The contribution
1319 of color to motion processing in macaque middle temporal area. 1320
Journal of Neuroscience, *19*, 6571–6587, [http://www.jneurosci.org/
1321 cgi/content/full/19/15/6571](http://www.jneurosci.org/cgi/content/full/19/15/6571). [PubMed] [Article] 1322
- Thiele, A., Dobkins, K. R., & Albright, T. D. (2001). Neural correlates
1323 of chromatic motion perception. *Neuron*, *32*, 351–358, doi:10.1016/
1324 S0896-6273(01)00463-9. [PubMed] [Article] 1325
- Treutwein, B. (1995). Adaptive psychophysical procedures. *Vision*
1326 *Research*, *35*, 2503–2522, doi:10.1016/0042-6989(95)00016-S. 1327
- [PubMed] [Article] 1328
- Van Essen, D. C., Maunsell, J. H. R., & Bixby, J. L. (1981). The
1329 middle temporal visual area in the macaque: Myeloarchitecture, 1330
connections, functional properties and topographic organization. 1331
Journal of Comparative Neurology, *199*, 293–326. [PubMed] 1332
- Wandell, B. A. (1995). *Foundations of vision. Appendix B: Monitor*
1333 *calibration*. Sunderland, MA: Sinauer Press. 1334
- Wandell, B. A., Poirson, A. B., Newsome, W. T., Baseler, H. A.,
1335 Boynton, G. M., Huk, A., Gandhi, S., & Sharpe, L. T. (1999). 1336
Color signals in human motion-selective cortex. *Neuron*, *24*, 901–
1337 909, [http://www.neuron.org/content/article/fulltext?uid=
1338 PIIS0896627399440378](http://www.neuron.org/content/article/fulltext?uid=PIIS0896627399440378). [PubMed] [Article] 1339
- Yeh, T., Lee, B. B., & Kremers, J. (1996). The time course of
1340 adaptation in macaque retinal ganglion cells. *Vision Research*, *36*, 1341
913–931, doi:10.1016/0042-6989(95)00332-0. [PubMed] [Article] 1342
- Zeki, S. M. (1974). Functional organization of a visual area in the
1343 posterior bank of the superior temporal sulcus of the rhesus 1344
monkey. *Journal of Physiology*, *236*, 549–573. [PubMed] 1345
- Zeki, S. M. (1976). The functional organizations of projections from
1346 striate to prestriate visual cortex in the rhesus monkey. *Cold Spring*
1347 *Harbor Symposium on Quantitative Biology*, *40*, 591–600. [PubMed] 1348
- Zeki, S. M. (1978a). Functional specialisation in the visual cortex of
1349 the rhesus monkey. *Nature*, *274*, 423–428. [PubMed] 1350
- Zeki, S. M. (1978b). Uniformity and diversity of structure and function
1351 in rhesus monkey prestriate visual cortex. *Journal of Physiology*, *277*,
1352 273–290. [PubMed] 1353
- Zeki, S., Watson, J. D., Lueck, C. J., Friston, K. J., Kennard, C., &
1354 Frackowiak, R. S. (1991). A direct demonstration of functional 1355
specialization in human visual cortex. *Journal of Neuroscience*, *11*, 1356
641–649, <http://www.jneurosci.org/cgi/reprint/11/3/641>. [PubMed] 1357
- [Article] 1358

AUTHOR QUERY FORM

AUTHOR PLEASE ANSWER ALL QUERIES

AQ1: “Area MT” was changed to “middle temporal area.” Okay?

AQ2: LGN was defined as lateral geniculate nucleus. Correct?

AQ3: The reference to Sincich & Horton, 2004, was changed to Sincich et al., 2004. Okay?